ELSEVIER

Mathematical Biosciences 168 (2000) 77–115

Mathematical Biosciences

www.elsevier.com/locate/mbs

A mathematical model for the roles of pericytes and macrophages in the initiation of angiogenesis. I. The role of protease inhibitors in preventing angiogenesis ☆

Howard A. Levine [a], Brian D. Sleeman [b,*], Marit Nilsen-Hamilton [c]

[a] *Department of Mathematics, Iowa State University, Ames, Iowa 50011, USA*
[b] *Department of Applied Mathematics, School of Mathematics, University of Leeds, Leeds LS2 9JT, UK*
[c] *Department of Biochemistry, Biophysics and Molecular Biology, Iowa State University, Ames, Iowa 50011, USA*

Received 16 July 1999; received in revised form 19 June 2000; accepted 20 June 2000

Abstract

In this paper, a simple mathematical model developed in H.A. Levine, B.D. Sleeman, M. Nilsen-Hamilton [J. Math. Biol., in press] to describe the initiation of capillary formation in tumor angiogenesis is extended to include the roles of pericytes and macrophages in regulating angiogenesis. The model also allows for the presence of anti-angiogenic (angiostatic) factors. The model is based on the observation that angiostatin can prevent the degradation of fibronectin in the basal lamina by inhibiting the catalytic action of active proteolytic enzyme. That is, it is proposed that the inhibitor 'deactivates' the protease but that it does not reduce the over all concentration of the protease. It consequently explores the possibility of preventing neovascular capillaries from migrating through the extra-cellular matrix toward the tumor by inhibiting protease action. The model is based on the theory of reinforced random walks coupled with Michaelis–Menten mechanisms which view endothelial cell receptors as the catalysts for transforming both tumor and macrophage derived angiogenic factors into proteolytic enzyme which in turn degrade the basal lamina. A simple catalytic reaction is proposed for the degradation of the basal lamina by the active proteases. A mechanism, in which the angiostatin acts as a protease inhibitor is discussed which has been substantiated experimentally. A second mechanism for the production of protease inhibitor from angiostatin by endothelial cells is proposed to be of Michaelis–Menten type. Mathematically, this mechanism includes the former as a subcase.

Keywords: Angiogenesis; Tumor growth; Reinforced random walks; Michaelis–Menten enzyme kinetics; Angiostatins

☆ This work was supported in part by NATO grant CRG-95120 and by NSF grant DMS-98-03992.

* Corresonding author. Tel.: +44-113 233 5188; fax: +44-113 242 9925.
E-mail addresses: halevine@iastate.edu (H.A. Levine), bds@amsta.leeds.ac.uk (B.D. Sleeman), marit@iastate.edu (M. Nilsen-Hamilton).

0025-5564/00/$ - see front matter
PII: S0025-5564(00)00034-1

1. Introduction

Angiogenesis is the main feature of neovascularization, the formation of new blood vessels. It is defined as the outgrowth of new vessels from a pre-existing vascular network and is fundamental to the formation of blood vessels during placental growth and in wound healing, for example. In regard to tumor growth, angiogenesis is initiated by the release of certain angiogenic and/or chemotaxic factors from the tumor, an idea first proposed by Folkman. See his article in [8] for an elegant overview.

The relevant biology for the onset of angiogenesis is described as follows: endothelial cells (EC), which make up the lining of capillaries and other vessels [24] form a mono-layer of flattened and extended cells inside capillaries. The abluminal surface of the capillaries is covered by a collageneous network intermingled with laminin. This is called the basal lamina (BL). This layer is continuous and serves as a scaffold or exocytoskeleton upon which the EC can rest. The BL is mainly formed by the EC while layers of EC and BL are sheathed by fibroblasts and possibly smooth muscle cells. In the neighborhood of the BL, there are other cell types such as pericyte cells (PC), platelet, macrophage cells (MC) and mast cells. Of these, macrophages can be stimulated to release angiogenic factors which, in their turn, induce the aggregating EC to release proteolytic enzymes. Pericytes, as argued in [6], are derived from primitive mesenchymal cells and are involved in the regulation of the proliferation of EC. When they are in contact with EC, EC cell division is proposed to be inhibited. Indeed, no pericytes are present in regions in which a vigorous proliferative activity of EC can be observed.

In response to one or more angiogenic or chemotactic chemical stimuli (collectively called tumor angiogenic factors, TAFs [1]) the EC in nearby capillaries appear to thicken and produce proteolytic enzymes (proteases), which in turn degrade the basal lamina. In further response to the angiogenic factor, the normally smooth cell surface begins to develop foot-like structures (pseudopodia) that penetrate the weakened basal lamina into the extra cellular-matrix (ECM) [3,24]. The endothelial cells subsequently begin to accumulate in regions where the concentration of tumor angiogenic factor reaches a threshold concentration [24]. The vessel dilates as the EC aggregate and the proteases degrade the basal lamina and the ECM, thus enabling the capillary sprouts to migrate and grow toward the chemotactic source in a tumor cell colony [12,31]. In [18], a simple mathematical model was presented based on the theory of reinforced random walks [17,23] coupled with a Michaelis–Menten type mechanism which views the EC receptors as the catalyst for transforming angiogenic factor into proteolytic enzyme. This model was proposed as a mechanism to describe the changes within the existing vessel prior to capillary formation.

The numerical experiments with this model in [18] show that under the conditions of slow cell movement and high chemotactic sensitivity, an initially uniform distribution of endothelial cells will form a bimodal distribution. In [18], we also gave a theoretical explanation for the formation of such a bimodal distribution based upon our work in [17].

Biologically, bimodal distributions of epithelial cells occur in nature, for example during the fetal development of teats [1]. During the formation of mammary ducts, a sheet of epithelial cells on the

[1] We reserve the term VEGF, vascular endothelial cell growth factor, for the enzyme that the endothelial cells convert to protease.

surface of a fetus aggregate at the surface in a ring. The cells presumably emit a protease which breaks down the supporting surface. The cells form a small mound which then penetrates into the fetal interior when the supporting surface breaks down. This leads to the formation of the mammary duct.

In this paper, we propose an extension of the model developed in [18] that takes into account the fact that macrophages produce angiogenic factors in response to tumor-produced chemotaxic agent [8] and the role that PC play in the formation of new capillaries.

We are only attempting to model the *onset* of angiogenesis here. That is, we are only attempting to model the observations described in Figs. 1 and 2 [25]. We are currently extending this model to the ECM with the goal of modeling the observations Rakusan summarizes in Figs. 3 and 4. This model consists of one-dimensional cell transport and kinetic equations along the capillary coupled with two-dimensional cell transport and kinetic equations in the ECM between the tumor and the neighboring capillary. It is quite complicated even when one does not consider the motion of macrophage and PC along with the motion of the ECM. Our goal here is to carefully explore the issues involved in the onset of angiogenesis before presenting the full two- or three-dimensional model to the scientific community.

PC, which form a periendothelial cellular network within the basal lamina, are intimately involved in the regulation of the proliferation of endothelial cells. Although PC are absent in regions

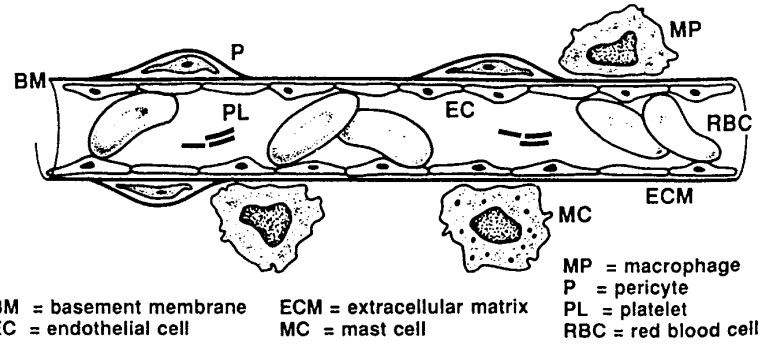

Fig. 1. Stage O of angiogenesis: stable vessel. Major components of normal stable capillary which can be involved in angiogenesis (from [25]).

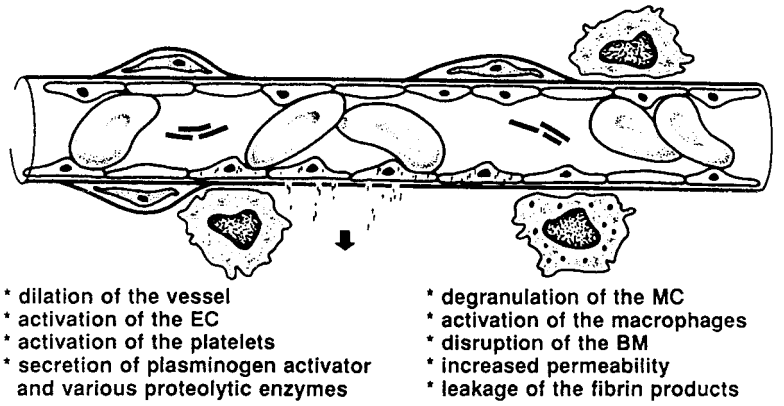

Fig. 2. Stage 1 of angiogenesis: changes within the existing vessel (from [25]).

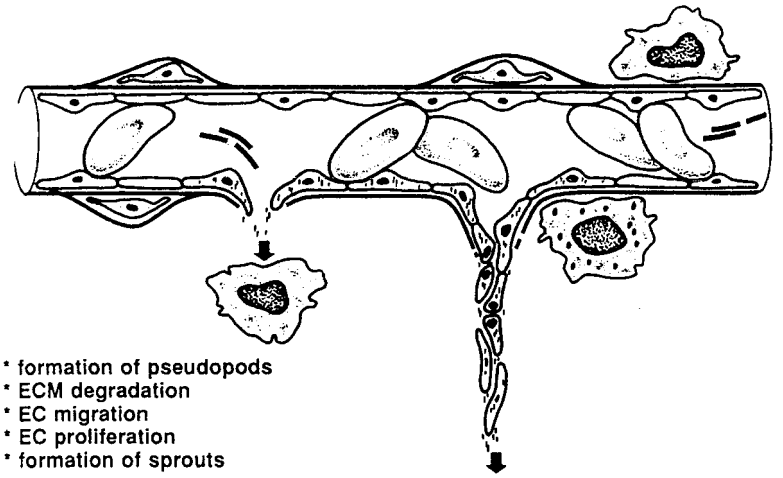

Fig. 3. Stage 2 of angiogenesis: formation of a new channel (from [25]).

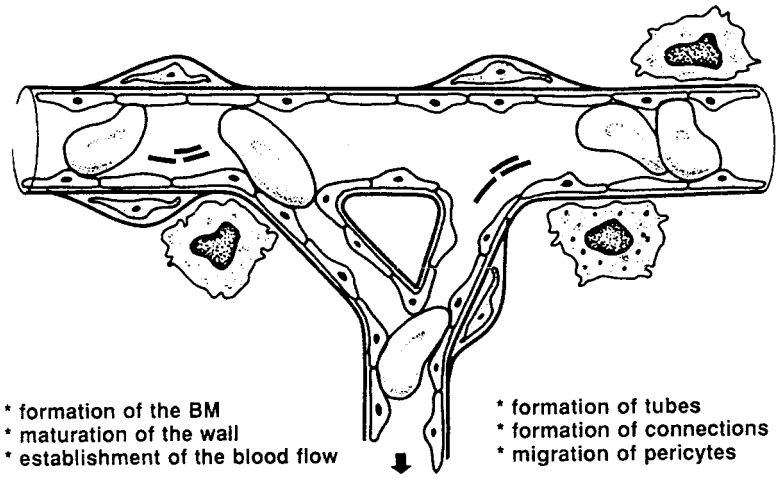

Fig. 4. Stage 3 of angiogenesis: maturation of the new vessel (from [25]).

of high endothelial cell proliferation activity, they are believed to have a 'managerial' role. As discussed in [30], angiogenesis is initiated most commonly from capillaries rich in pericytes. Indeed they present the thesis that during angiogenesis, newly formed capillaries are formed by both endothelial cells and pericytes.

Referring to Fig. 5(a) (taken from [8]) in [18], the mechanism for the onset of angiogenesis was the path $1 \to 2 \to 3$. Here, we incorporate the path $1 \to 5 \to 6 \to 3$ of Fig. 5(a). In a mathematical sense, the former path can be thought of as a subpath of the latter path. However, the angiogenic factors produced by the tumor are not necessarily the same as those produced by the MCs in response to the tumor necrotic factors (TNFs). In this way, we address the additional contribution to angiogenesis through tumor derived growth factors that are chemotactic for macrophages as well as addressing the mediating role of pericytes.

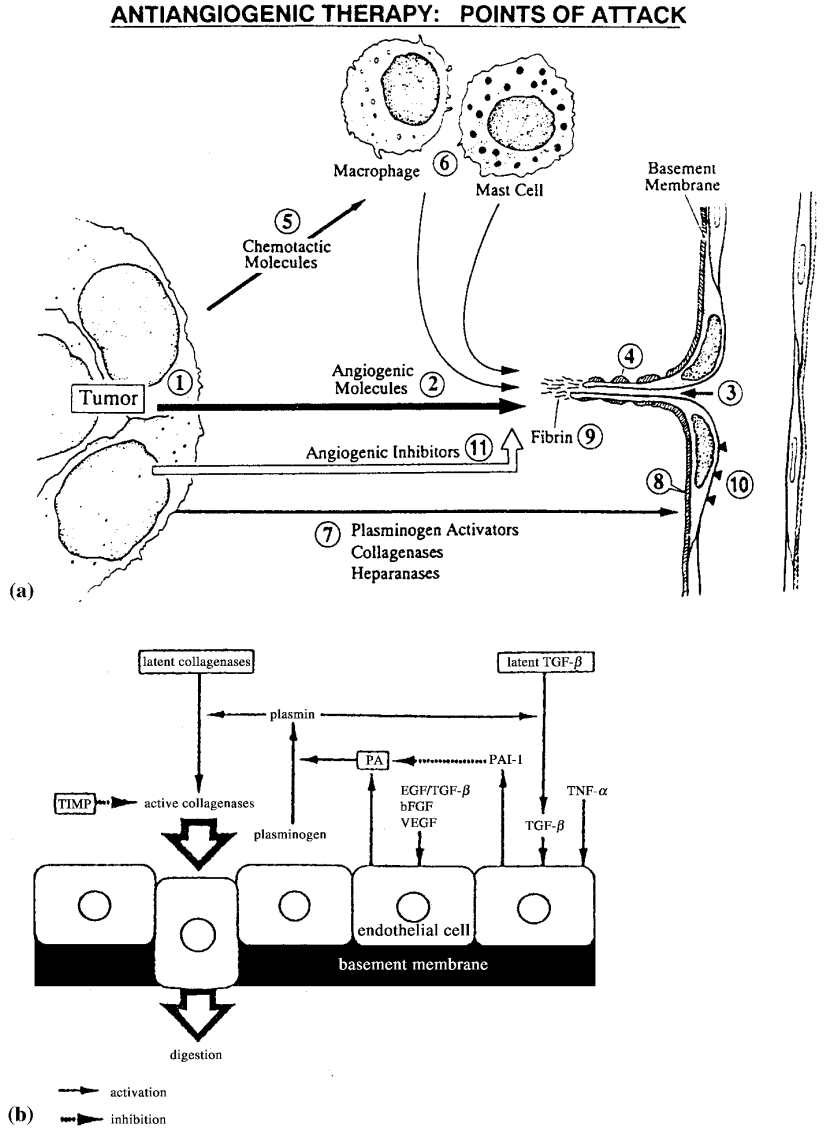

Fig. 5. (a) Diagram of different targets for antiangiogenic therapy (from [8]). (b) Expression of PA and its inhibitors in endothelial cells, and initiation of angiogenesis in model system. In this model, EGF/TGF-α, TGF-β, and TNF-α are potent factors in HOME cells, while a FGF/bFGF, VEGF, and TGF-β are potent in BAE and HUVE cells (from [15]).

The model we present here shows that the onset of angiogenesis also leads to a bimodal density distribution in *three* of the major cell types, endothelial cells, PCs and MCs, that are involved in capillary development and that are considered here.

As Folkman suggests, these paths can be viewed as points of attacks on angiogenesis in tumor growth. In this paper, we also propose two mechanisms for the action of angiostatic agents to inhibit tumor growth by inhibiting the onset of angiogenesis. (We distinguish between naturally occurring angiostatins and those that are pharmacologically applied. The former are byproducts

of the cleavage of plasminogin by this protease. Its role will be considered in a later paper. In this paper, we will use the term 'angiostatic agent' as a pseudonym for anti-angiogenic factors such as angiogenic steroids, which are introduced into the body as a therapeutic drug.) The rough idea is that in response to angiostatic agents, endothelial cells produce protease inhibitors which deactivate the protease formed by the endothelial cells in response to TAF. The protease is not destroyed but rather is prevented from functioning as a catalyst for the degradation of the basel lamina.

The biology of tumor angiogenesis is very complex and as such it is important to proceed in a logical fashion. That is, it is important to develop the model in stages and to build upon the biological and biochemical observations of cellular response to growth factors.

Mathematical modeling of angiogenesis has been discussed by a number of authors and we refer the reader to [2,22,26,29] for recent overviews. Most of the aspects of angiogenesis work has mainly concerned the growth of capillary branches and anastamosis within the ECM and do not address, in general, the initiation of capillary sprout formation. *This onset (and inhibition) of sprout formation is the main focus of our study here.* However, we remark that the early development of pre-initiated capillary sprouts has been modeled in [22]. In that model, the authors concentrated on the role of haptotaxis to regulate cell movement due to the release of fibronectin, which increases the cell to matrix adhesiveness and serves as a provisional matrix for subsequent growth and migration. That model is based on reaction–diffusion mechanisms and capillary sprout development is accounted for through Turing-diffusion driven instability.

The modeling approach developed in this paper, is, to the best of our knowledge, completely new. The basic equations of enzyme kinetics coupled with the equations of reinforced random walks govern the cell movements. The reinforcement factors (chemotactic, haptotactic) are assumed to be driven by EC-produced protease in response to growth factor, which is produced by MCs in response to some tumor-produced chemotactic agent induced by hypoxia, for example.

We believe the modeling procedure is robust and sufficiently flexible to incorporate further growth and inhibiting factors known, or likely to be of importance in developing a deeper understanding of angiogenesis.

One early criticism of our model was that we did not have available to us reliable sensitivity coefficients as well as certain cell movement constants and reaction rate constants. However, we now have a good set of approximate values for the cell movement constants and the reaction rate constants. The values we use in our computations here are typical of the values we have found in the literature upon non-dimensionalization of our equations [16]. The sensitivity constants must be obtained empirically.

Mathematically, the sensitivity coefficients determine the relative amount of cell aggregation or de-aggregation. These have yet to be determined experimentally.

The plan of the paper is as follows: in Section 2, we model the kinetics of the chemotactic and angiogenic factors produced by the tumor and MCs. First, we employ Michaelis–Menten kinetics to model the conversion of the tumor chemotactic factor by macrophages into angiogenic factor. (Path $1 \to 5$ in Fig. 5(a).) Then, we employ this type of kinetics a second time to model the conversion of the macrophage generated angiogenic factor into protease by endothelial cells. (Path $5 \to 6$ in Fig. 5(a).) Protease is then viewed as a catalyst in a reaction for the degradation of fibronectin, first in the basal lamina, and subsequently in the ECM itself. The endothelial cells which line the capillary then migrate through the wall of the capillary along the trail of angiogenic

molecules toward the tumor. (As remarked above, the growth factor transport across the ECM and the capillary growth in the opposite direction will appear in [16].)

One novel aspect of our work is the inclusion of two mechanisms for the action of angiostatic agent as an inhibitor of the protease catalysis. This is an important objective of the modeling. Such mechanisms show how angiostatic agents are capable of acting to prevent fibronectin from being degraded. In doing so, it supports the use of anti-angiogenic drugs as a possible clinical therapy to combat tumor growth and metastasis.

In Section 3, the movement of EC, PCs and MC (MCs) is modeled using the notion of reinforced random walks. In [18], we used this idea to model the movement of EC in the capillary. The rough idea is that endothelial cell movement is envisioned to be toward regions in which there are large concentrations of protease and low concentrations of fibronectin. That is, these cells move *up* the concentration gradients of protease and *down* the concentration gradients of fibronectin. Likewise the movement of PCs based on the observations that PCs move *up* a fibronectin gradient while macrophages will move *up* the concentration gradient of the tumor emitted chemotactic factor. Simple models of probability transition functions are then taken to model these movements.

In Section 4, we discuss the resulting system from the point of view of the theory we developed in [17]. In Section 5, we present some computations which illustrate the significance of the model. Finally, in Section 7, we discuss our findings and indicate the future directions of this research.

2. Biochemical kinetics

In order to better understand how tumor-generated angiogenic factors act on endothelial cells, we consider a simplified version of Fig. 5(b) (taken from [15]). That is, we consider that each endothelial cell has a certain number of receptors to which the angiogenic factor (ligand) binds. The bound molecules (intermediates) in turn stimulate the cell to produce proteolytic enzyme and form new receptors.

In the case of MCs, we use the fact that they produce an angiogenic factor in response to a chemotactic agent produced by the tumor. This chemotactic agent then binds with endothelial cells in much the same way as described in the preceding paragraph.

2.1. The role of tumor-generated angiogenic factor in protease production

Let V_T be the angiogenic factor produced by the tumor and V_M that produced by macrophages which are stimulated by a chemotaxic agent K.

We model the process for tumor-produced angiogenic factor as follows:

$$V_T + R_E \underset{k_{-1}}{\overset{k_1}{\rightleftarrows}} [R_E V_T],$$

$$[R_E V_T] \xrightarrow{k_2} C_T + R_E,$$

where R_E denotes some receptor site on the endothelial cell surface membrane, $[R_E V_T]$ is the intermediate and C_T is a proteolytic enzyme produced as a consequence of this reaction. (Actually the angiogenic factor binds to the receptor at the surface of the cell. The complex is then carried to the interior of the cell, where it stimulates the production of proteases and R_E, which then moves

to the cell surface. The point of view here is that the receptors at the surface of the cell function play the same role that enzymes play in the classical enzymatic catalysis.)

2.2. The role of tumor-generated chemotaxic factors in enzyme kinetics

Here we envisage, in accordance with [8], that the tumor releases a chemotactic agent, K, which attracts the macrophages. The macrophages 'convert' the chemotactic agent into an angiogenic factor V_M according to the following mechanism:

$$\begin{aligned} &K + R_{Ma} \underset{k_{-3}}{\overset{k_3}{\rightleftarrows}} [R_{Ma}K], \\ &[R_{Ma}K] \xrightarrow{k_4} V_M + R_{Ma}, \end{aligned} \tag{2.2.1}$$

where R_{Ma} is a receptor site on the MC wall and $[R_{Ma}K]$ is the intermediate complex that is taken into the macrophage and stimulates the production of angiogenic factor.

This factor, in turn, stimulates the production of a proteolytic enzyme C_M by the endothelial cells by much the same mechanism as in the earlier case:

$$\begin{aligned} &V_M + R'_E \underset{k'_{-1}}{\overset{k'_1}{\rightleftarrows}} [R'_E V_M], \\ &[R'_E V_M] \xrightarrow{k'_2} C_M + R'_E. \end{aligned} \tag{2.2.2}$$

Regardless of whether the proteolytic enzyme is produced by TAF (C_T) or secondarily by macrophage-generated angiogenic factor (C_M), we assume that it acts to degrade fibronectin (F) via the Michealis–Menten catalytic reaction:

$$\begin{aligned} &C_A + F \xrightarrow{k_7} [FC_A], \\ &[FC_A] \xrightarrow{k_8} F' + C_A. \end{aligned} \tag{2.2.3}$$

In this reaction, C_A refers only to those molecules of proteolytic enzyme (C_M or C_T) that are actually involved in the degradation of fibronectin. [2] The reaction Eq. (2.2.3) reflects the fact that the enzyme degrades the fibronectin, converting it into products F', by means of catalysis.

Remark 1. It is to be emphasized that while the chemotactic agents K, V_T and V_M diffuse through the ECM from the MCs and the tumor, respectively, they are converted almost immediately into receptor complexes upon arrival at the capillary wall via the above reactions. In particular, chemotactic factor and growth factor are converted almost immediately into their respective activated receptor complex upon arrival at the capillary wall via the above reactions so that very little if any of it is left to diffuse along the capillary lumen. [3] Therefore, we might expect that the diffusion of these proteins along the length of the capillary lumen is negligible in comparison to

[2] An alternate mechanism for the degradation of fibronectin by plasmin, generated from plasminogen via protease, will be discussed in a forthcoming paper.

[3] This assumes that the rate of supply of the chemotactic factor at the wall is insufficient to saturate all of the available macrophage receptors and that the quantities of growth factor so generated by the MC are likewise insufficient to saturate all or nearly all the available EC receptors.

their conversion into receptor complex. (A mathematical justification for this is given in Appendix A. We also include a computation that illustrates this.) Likewise, angiostatin is presumed to be converted into inhibitor which in turn effectively binds with active enzyme more rapidly than it can diffuse along the capillary wall.

The diffusion of these proteins cannot be neglected in the ECM in the full model we are developing in [16], since diffusion is the transport mechanism for these proteins to and from the tumor. However, at the capillary wall, diffusion of these proteins is far less important than their interaction with the endothelial cells.

2.3. Models for the action of angiostatins

There are perhaps several ways in which angiostatic agents might inhibit angiogenesis [10,14]. Here, we discuss two possibilities, at least one of which has been verified in the experimental literature. We begin with this mechanism.

We consider the angiostatin as a direct inhibitor of protease. When we do this,

$$A + C_A \rightleftarrows C_I. \tag{2.3.1}$$

Here, C_I denotes the proteolytic enzyme molecules which are inhibited by the inhibitor A from functioning as a catalyst for fibronectin degradation. In terms of concentrations, $[C] = [C_A] + [C_I]$. Assuming that (2.3.1) is in equilibrium, we have that $[C_I] = v_e[A][C_A]$, where v_e is the equilibrium constant for this step. In general, the reaction in (2.3.1) will be essentially complete if $v_e \gg 1$. Justification for this mechanism is to be found in [27], where plasminogen activation is shown to be inhibited by angiostatin. The tissue plasminogen activator (tPA) is produced in response to a growth factor such as VEGF. Then, tPA binds to plasminogen with the resultant product being plasmin (Pm). In the model proposed in [27], the angiostatin binds directly to the intermediate [tPA–Pg] complex to inhibit the production of active protease. (The angiostatin here is a fragment of plasminogen with a molecular weight of about 38 kDa.) The literature value in [27] given for v_e^{-1} is of the order of 1 μM. Thus, in this example we cannot assume that (2.3.1) is essentially complete.

Another possibility is to involve the endothelial cells once more. In this more complex mechanism, the angiostatin stimulates EC to produce an inhibitor I according to the mechanism

$$\begin{aligned} &A + R_{EA} \underset{k'_{-5}}{\overset{k'_5}{\rightleftarrows}} [AR_{EA}], \\ &[AR_{EA}] \overset{k'_6}{\rightarrow} I + R_{EA}, \\ &C_A + I \rightleftarrows C_I, \end{aligned} \tag{2.3.2}$$

where R_{EA} is a receptor protein on the endothelial cell wall and $[AR_{EA}]$ is the intermediate complex. Moreover, I is a protease inhibitor produced by the endothelial cells in response to the angiostatic agent by an overall mechanism, which we will assume to be of Michealis–Menten type also. Here, C_I denotes the proteolytic enzyme molecules which are inhibited by the inhibitor I from functioning as a catalyst for fibronectin degradation. In terms of concentrations, $[C] = [C_A] + [C_I]$. Assuming that the last step in (2.3.2) is in equilibrium, we have that $[C_I] = v_e[I][C_A]$, where v_e is the equilibrium constant for this step. In general, it will be quite large, that is, the last step in (2.3.2) is essentially complete.

In either case, the critical equation for the concentration of active enzyme is

$$[C_A] = \frac{[C]}{1 + v_e[J]},$$

where $J = A$ if the angiostatin is the inhibitor or $J = I$ if the angiostatin generates inhibitor via (2.3.2). [4]

Remark 2. The models we propose here for the action of an angiostatic agent are only two of several possible models. There are others which we intend to investigate in a series of papers of which this is the second. It is probably better to treat each model separately rather than to combine them all into one grand 'unified theory' because of the complex nature of the underlying biology and biochemistry.

We mention here just a few of the possibilities we plan to explore in the future:

1. Angiogenesis inhibitors that inhibit EC from invading the ECM.
2. Angiogenesis inhibitors that inhibit proliferation of endothelial cells.
3. Angiogenesis inhibitors that block growth factor receptors.

(This is a partial list taken from [20].) The long-term goal is to determine mathematically which model or combination of models might most effectively describe angiogenesis.

2.4. The kinetic equations

Whether the macrophages produce the same angiogenic factor that the tumor produces is an open question. Also open to debate is whether the enzyme C_M is the same as C_T. In the interest of mathematical simplicity, we shall make these assumptions. Then, we take $k_i' = k_i$ for $i = -1, 1, 2$, $\mu_i' = \mu_i$ for $i = 1, 2$, $R_E = R_E'$ and $V_T = V_M$. (The receptor for the angiostatic agent, R_{EA} is not assumed to be the same as for the angiogenic factor. Otherwise the nine differential equations we solve numerically below, blossom into eleven equations.) The tumor supplied angiogenic factor is then viewed as an initial condition at the BL. Thus we consider the simplified system of cellular reactions

$$\begin{aligned}
K + R_{Ma} &\underset{k_{-3}}{\overset{k_3}{\rightleftarrows}} [R_{Ma}K],\\
[R_{Ma}K] &\xrightarrow{k_4} V + R_{Ma},\\
V + R_E &\underset{k_{-1}}{\overset{k_1}{\rightleftarrows}} [R_E V],\\
[R_E V] &\xrightarrow{k_2} C + R_E,\\
A + R_{EA} &\underset{k_{-5}}{\overset{k_5}{\rightleftarrows}} [AR_{EA}],\\
[AR_{EA}] &\xrightarrow{k_6} I + R_{EA},\\
C_A + I &\rightleftarrows C_I
\end{aligned} \tag{2.4.1}$$

[4] While we do not have rate constants involved in (2.3.2), we do have rate constants for the VEGF-protease system (2.2.2). We shall assume that the rate constants for the former are roughly of the same order of magnitude as those of the latter in our illustrative computations below.

in addition to the fibronectin – enzyme decay mechanism (2.2.3). We understand that in the mechanism in which angiostatin is the inhibitor, the mechanism becomes

$$\begin{aligned} &K + R_{\mathrm{Ma}} \underset{k_{-3}}{\overset{k_3}{\rightleftarrows}} [R_{\mathrm{Ma}}K], \\ &[R_{\mathrm{Ma}}K] \xrightarrow{k_4} V + R_{\mathrm{Ma}}, \\ &V + R_{\mathrm{E}} \underset{k_{-1}}{\overset{k_1}{\rightleftarrows}} [R_{\mathrm{E}}V], \\ &[R_{\mathrm{E}}V] \xrightarrow{k_2} C + R_{\mathrm{E}}, \\ &C_{\mathrm{A}} + A \rightleftarrows C_{\mathrm{I}}. \end{aligned} \tag{2.4.2}$$

We imagine a basal lamina located on some interval $[0, L]$ of the x-axis. Then, the densities and concentrations of cell tissues and the chemical species are functions of position and time (in units of micromolarity or micromoles per unit liter) and their time rates of change are denoted by $\partial/\partial t$. We adopt the following notation for these functions:

$$\begin{aligned} &u = \text{concentration of chemotactic agent } K, \\ &v = \text{concentration of angiogenic factor } V_{\mathrm{T}} \text{ (taken to be that of } V_{\mathrm{M}} \text{ here)}, \\ &c = \text{concentration of proteolytic enzyme } C_{\mathrm{T}}, \text{ (taken to be that of } C_{\mathrm{M}} \text{ here)}, \\ &r = \text{density of angiogenic response receptors, } R_{\mathrm{E}}, \text{ on the EC cells}, \\ &r_{\mathrm{a}} = \text{density of angiostatic agent receptors, } R_{\mathrm{EA}}, \text{ on the EC cells}, \\ &r_m = \text{density of receptors, } R_{\mathrm{Ma}}, \text{ on the MCs}, \\ &\ell = \text{concentration of intermediate receptor complex } [R_{\mathrm{E}}V_{\mathrm{T}}] = [R_{\mathrm{EV}}], \\ &\ell_{\mathrm{a}} = \text{concentration of intermediate receptor complex } [AR_{\mathrm{EA}}], \\ &\ell_m = \text{concentration of intermediate receptor complex } [R_{\mathrm{Ma}}K], \\ &f = \text{density of capillary wall, represented by here by fibronectin}, \\ &a = \text{concentration of angiostatic agent (anti-angiogenic) factor}, \\ &\eta = \text{endothelial cell density}, \\ &\sigma = \text{PC density}, \\ &\iota_{\mathrm{a}} = \text{protease inhibitor density}, \\ &c_{\mathrm{a}} = \text{active proteolytic enzyme density}, \\ &c_{\mathrm{i}} = \text{inhibited proteolytic enzyme density}. \end{aligned} \tag{2.4.3}$$

We also have, in the case that angiostatin is the inhibitor,

$$\begin{aligned} &c = c_{\mathrm{a}} + c_{\mathrm{i}}, \\ &c_{\mathrm{i}} = v_{\mathrm{e}} a c_{\mathrm{a}} \end{aligned}$$

so that

$$c_{\mathrm{a}} = \frac{c}{1 + v_{\mathrm{e}} a},$$

while if angiostatin is an inhibitor substrate,

$$\begin{aligned} c &= c_{\mathrm{a}} + c_{\mathrm{i}}, \\ c_{\mathrm{i}} &= v_{\mathrm{e}} \imath_{\mathrm{a}} c_{\mathrm{a}} \end{aligned} \tag{2.4.4}$$

so that

$$c_{\mathrm{a}} = \frac{c}{1 + v_{\mathrm{e}} \imath_{\mathrm{a}}}.$$

If we apply the law of mass action to (2.4.1), then we obtain

$$\begin{aligned} \frac{\partial u}{\partial t} &= -k_3 r_m u + k_{-3} \ell_m, \\ \frac{\partial r_m}{\partial t} &= -k_3 r_m u + (k_{-3} + k_4) \ell_m, \\ \frac{\partial \ell_m}{\partial t} &= k_3 r_m u - (k_{-3} + k_4) \ell_m, \\ \frac{\partial v}{\partial t} &= k_4 \ell_m - k_1 r v + k_{-1} \ell, \\ \frac{\partial r}{\partial t} &= -k_1 r v + (k_{-1} + k_2) \ell, \\ \frac{\partial \ell}{\partial t} &= k_1 r v - (k_{-1} + k_2) \ell, \\ \frac{\partial c}{\partial t} &= k_2 \ell, \\ \frac{\partial a}{\partial t} &= k_{-5} \ell_a - k_5 a r_{\mathrm{a}}, \\ \frac{\partial r_{\mathrm{a}}}{\partial t} &= -k_5 a r_{\mathrm{a}} + (k_{-5} + k_6) \ell_{\mathrm{a}}, \\ \frac{\partial \ell_{\mathrm{a}}}{\partial t} &= k_5 a r_{\mathrm{a}} - (k_{-5} + k_6) \ell_{\mathrm{a}}, \\ \frac{\partial \imath_{\mathrm{a}}}{\partial t} &= k_6 \ell_{\mathrm{a}}. \end{aligned} \tag{2.4.5}$$

In the case of the mechanism (2.4.2), we agree to delete the last three equations of this system. The rate equation for $a(x,t)$ will be included in a somewhat different form but not with the kinetic constants $k_{\pm 5}$.

Applying standard Michealis–Menten enzyme kinetics to (2.2.3), we have

$$\frac{\partial f}{\partial t} = -\frac{\lambda_4 c_{\mathrm{a}} f}{1 + v_4 f}, \tag{2.4.6}$$

where $\lambda_4 = k_8$ and $v_4 = k_8/k_7$. [5]

[5] The units of the k_{2i} are in reciprocal hours and of the k_{2i-1} are reciprocal hours per μM (1 μM = 1 micromole per liter).

The rate equations for fibronectin and for protease are not complete as they stand. For example, it is known that protease decays at a rate proportional to its concentration. This means that the seventh of Eqs. (2.4.5) should have the form

$$\frac{\partial c}{\partial t} = k_2 \ell - \mu c, \tag{2.4.7}$$

where μ is a decay constant. For the remainder of this paper, we shall take $\mu = 0$ as a 'worst case' scenario. This simplifies the analytical discussion to follow somewhat and does not significantly affect the numerical computations which follow that discussion. (We should perhaps add here that the decay constant μ is available for some proteases in vitro at elevated temperatures or other unusual environmental conditions. The values for the types of in vivo proteases that we have in mind do not seem to be available.) [6]

In so far as the rate equation for fibronectin is concerned, it is known that the endothelial cells can also produce fibronectin. Therefore, the rate law for the fibronectin assumes the form

$$\frac{\partial f}{\partial t} = \beta(f_{\mathrm{M}} - f) f \eta - \frac{\lambda_4 c_{\mathrm{a}} f}{1 + \nu_4 f}, \tag{2.4.8}$$

where f_{M} is some maximal value for the fibronectin. That is, once f reaches f_{M}, the endothelial cells cease their production of fibronectin.

Initially, there are no receptor–ligand complexes. Therefore, $\ell_m(x,0) = \ell(x,0) = \ell_{\mathrm{a}}(x,0) = 0$. We see from the second, third, fourth, fifth, ninth and tenth of (2.4.5) after a quadrature that

$$\begin{aligned} &r_m(x,t) + \ell_m(x,t) = r_m(x,0), \\ &r(x,t) + \ell(x,t) = r(x,0), \\ &r_{\mathrm{a}}(x,t) + \ell_{\mathrm{a}}(x,t) = r_{\mathrm{a}}(x,0). \end{aligned} \tag{2.4.9}$$

If, as in the usual Michealis–Menten hypothesis ([19]), we set $\partial_t r_m/k_1 = \partial_t r/k_3 = \partial_t r_{\mathrm{a}}/k_5 = 0$, there results

$$\begin{aligned} r_m(x,t) &= \frac{r_m(x,0)}{1 + \nu_2 u(x,t)}, \\ \ell_m(x,t) &= \frac{\nu_2 r_m(x,0) u(x,t)}{1 + \nu_2 u(x,t)}, \\ r(x,t) &= \frac{r(x,0)}{1 + \nu_1 v(x,t)}, \\ \ell(x,t) &= \frac{\nu_1 r(x,0) v(x,t)}{1 + \nu_1 v(x,t)}, \end{aligned} \tag{2.4.10}$$

[6] It should be remarked that in the work we have under way, where we consider the actual penetration of the capillary sprout into the ECM, this term will play a critical role. The reason for this is that in the ECM the EC cell proliferation rate and EC death rate are not in balance. This means that the EC cell movement equation must include a source term of the form $NG'(C)C_t/(1 + G(C)) + \kappa_1 N(N_0 - N) - \kappa_2 N$, where $N(x,y,t)$ (resp. $(N(x,y,z,t))$ is the two- (resp. three-) dimensional EC cell density and $G(c)$ is a biphasic EC mitosis rate term, which decays to zero as $c \to +\infty$. The inclusion of the term μc in the enzyme rate law prevents $c \to +\infty$. Further discussion of this here would take us beyond the scope of the present paper.)

$$r_a(x,t) = \frac{r_a(x,0)}{1+v_3 a(x,t)},$$
$$\ell_a(x,t) = \frac{v_3 r_a(x,0) a(x,t)}{1+v_3 a(x,t),}$$

where we have set $v_i = k_{2i-1}/(k_{-(2i-1)} + k_{2i})$ for $i = 1,2,3$.

Mathematically speaking, these equations cannot be correct as they stand. Consider for example, the first of (2.4.10). This cannot hold at $t = 0$ unless the initial concentration of chemotactic factor is zero. Of course, as pointed out in Murray [19, ch. 5], this difficulty arises because the assumptions that $1/(k_1 r_m(x,0)) = 1/(k_3 r(x,0)) = 1/(k_5 r_a(x,0)) = 0$ are not consistent with the number of initial conditions for the system (2.4.5). In other words, we are dealing with a singular perturbation problem here. Eqs. (2.4.10) are only valid in deriving the so-called 'outer solution'. The outer solution is considered to be valid only for times $t \gg \epsilon = \max\{1/(k_3 r_m(x,0)), 1/(k_1 r(x,0)), 1/(k_5 r_a(x,0))\}$ and must be matched with the so-called 'inner solution'. Murray does this in [19]. Murray refers to the outer solution as the 'pseudo steady state'. He also uses a singular perturbation argument to give a set of circumstances under which (2.4.10) may be justified. If ϵ is very small, then we need only concern ourselves with the outer solution. [7]

Using (2.4.10) in the equations for $\partial_t u$, $\partial_t v$, $\partial_t c$, $\partial_t a$ and $\partial_t \iota_a$ in (2.4.5), we find that for $t \gg \epsilon$

$$\begin{aligned}
\frac{\partial u}{\partial t} &= -\frac{v_2 k_4 u r_m(x,0)}{1+v_2 u},\\
\frac{\partial v}{\partial t} &= \frac{v_2 k_4 u r_m(x,0)}{1+v_2 u} - \frac{v_1 k_2 v r(x,0)}{1+v_1 v},\\
\frac{\partial c}{\partial t} &= \frac{v_1 k_2 v r(x,0)}{1+v_1 v},\\
\frac{\partial a}{\partial t} &= -\frac{v_3 k_6 a r_a(x,0)}{1+v_3 a},\\
\frac{\partial \iota_a}{\partial t} &= \frac{v_3 k_6 a r_a(x,0)}{1+v_3 a}.
\end{aligned} \tag{2.4.11}$$

We would like to replace $r_m(x,0)$ by $r_m(x,t)$, $r(x,0)$ by $r(x,t)$ and $r_a(x,0)$ by $r_a(x,t)$ and ultimately by $m(x,t)$ and $\eta(x,t)$. The argument we make to justify this is based on the pseudo steady-state approximation discussed in [19, p. 119].

We observe from the first and fourth of these that u, a must decay exponentially fast since they are decreasing functions of time. [8] It then follows from the second of these equations that v must ultimately vanish. [9] For if v had a sequence of positive maxima as $t \to +\infty$ and these maximum values were bounded away from zero, then the second term on the right of the equation for v_t

[7] For example, using data from [13] for VEGF receptor KDR tyrosine kinase, $v_1 k_2 = K_{cat}/K_m$ and the approximation justified below that $r(x,0) \approx 1$ μM, we have that $1/(r(x,0)k_1) \approx 50$ s. Similar estimates should hold for $1/(k_3 r_m(x,0))$ and $1/(k_5 r_a(x,0))$.

[8] Implicit in this statement is the assumption that for each x, $r(x,0)$ and $r_a(x,0)$ are strictly positive. Thus, for example, the equation for u_t can be written as $u_t \leqslant -\delta(x)u$, where $\delta(x) = v_2 k_4 r(x,0/(1+u(x,0) > 0$. Therefore, $u(x,t) \leqslant \exp(-t\delta(x))$.

[9] That is, $\lim_{t\to+\infty} v(x,t) = 0$.

would be bounded away from zero from above while the first term on the right for v_t would tend to zero. This means that v_t would be negative in a neighborhood of a maximum which is of course nonsense.

Once we have assured ourselves that v decays, it is easy to see from the second equation that v also decays exponentially fast. If the decay of v is slower than an exponential, then the first term will ultimately be negligible in comparison with the second term. But then the resulting equation is of the same form as the first equation (with v in place of u) and hence v too must decay exponentially fast. (The fact that we have exponential decay of these quantities suggests that we may neglect their diffusion. See Appendix A.)

Thus, $\ell_m(x,t)$, $\ell(x,t)$ and $\ell_a(x,t)$ decay to zero exponentially. In view of the conservation laws (2.4.9) this means that for large times, the positive quantities $r_m(x,0) - r_m(x,t)$, $r(x,0) - r(x,t)$, and $r_a(x,0) - r_a(x,t)$ are all very small. (Indeed, in view of (2.4.10) these quantities decrease to zero like u^2, v^2 and a^2.) Thus, it is reasonable to replace $r_m(x,0)$ by $r_m(x,t)$, $r(x,0)$ by $r(x,t)$ and $r_a(x,0)$ by $r_a(x,t)$. This leads us to

$$\begin{aligned}
\frac{\partial u}{\partial t} &= -\frac{v_2 k_4 u r_m(x,t)}{1+v_2 u},\\
\frac{\partial v}{\partial t} &= \frac{v_2 k_4 u r_m(x,t)}{1+v_2 u} - \frac{v_1 k_2 v r(x,t)}{1+v_1 v},\\
\frac{\partial c}{\partial t} &= \frac{v_1 k_2 v r(x,t)}{1+v_1 v},\\
\frac{\partial a}{\partial t} &= -\frac{v_3 k_6 a r_a(x,t)}{1+v_3 a},\\
\frac{\partial \iota_a}{\partial t} &= \frac{v_3 k_6 a r_a(x,t)}{1+v_3 a}.
\end{aligned} \tag{2.4.12}$$

Finally, we would like to replace $r(x,t)$ and $r_a(x,t)$ by (some multiple of) $\eta(x,t)$ and $r_m(x,t)$ by $m(x,t)$ in the above equations. We need to do this because, while we have good estimates of the number of receptors per cell, it is the number of cells per unit length which we can, in principle, directly observe in sections of tissue under the microscope. We can write $r(x,t) = \delta(x,t)\eta(x,t)$, where δ, the number of receptors per cell, is taken to be nearly constant, although it may vary somewhat with η. In turn, this linear cell density must be converted to a volumetric density expressed in micromoles per liter. [10]

To find the volumetric density, we imagine the cells to be small rectangular parallelepipeds. Since capillaries have a diameter of about 6–8 μm and red blood cells have a diameter of 4–5 μm, we can estimate the thickness of an endothelial cell to be about 1 μm with a width of about $7\pi/2 \approx 10$ μm. (The thickness of the basal lamina itself is much smaller than that of an EC and is neglected.) It is known that there are about 10–100 EC per millimeter so that their length can be taken to be between 10 and 100 μm. This means that the volumetric density of endothelial cells is roughly of the

[10] The issue of units is quite important. In order to relate the constants to literature values where the terminology, K_{cat}, K_m is used, the concentrations of the chemical species in (2.4.12) must be expressed in volumetric units, say in micromoles per liter.

order of 10^{12} cells per liter. (The dimensions of an endothelial cell are taken from [21].) The number of receptors per cell is of the order of 10^5 [4,34]. Therefore, for the purposes of this model the receptor density is viewed as a concentration $\delta\eta_0 \approx 10^{17}$ per liter or 10^{-6} M or one μM.

(In the same manner, the receptor per cell ratios, $\delta_m(x,t) = r_m(x,t)/m(x,t)$ and $\delta_a(x,t) = r_a(x,t)/\eta(x,t)$ are assumed to be nearly constant and the micromolarity of available receptors of each type, $r_m(x,0)$ and $r_a(x,0)$, are of order 1 micromolar unit.)

We set $\lambda_i = \delta_i v_i k_{2i}$, where $\delta_1 = \delta,\ \delta_2 = \delta_m,\ \delta_3 = \delta_a$ and $\delta_4 = 1$. [11]

Before using this observation, we make a final comment.

Remark 3. The rate laws for the chemical mechanisms above must include terms that take into account tumor emitted angiogenic factor and chemotactic factor as proposed by Folkman [8]. That is, we envisage each of these factors as being supplied from the tumor to the wall at some (as yet unknown) rate $u_r(x,t)$ and $v_r(x,t)$, respectively. However, simple models for these rate functions can be written down. This we do later.

On the other hand, for therapeutic purposes, any angiostatic factor must be supplied at a rate, $a_r(x,t)$, sufficient to 'neutralize' the proteolytic enzyme until the tumor has been rendered inactive. A reasonable model for a_r might be a constant function since this factor could be supplied intravenously at a constant rate.

Therefore, the rate laws must include as source terms $u_r(x,t)$, $v_r(x,t)$ and $a_r(x,t)$, which drive this mechanism.

Thus, we ultimately obtain, noting the above remark, upon inclusion of (2.4.8), the following seven equations:

$$\begin{aligned}
\frac{\partial u}{\partial t} &= -\frac{\lambda_2 u m}{1+v_2 u} + u_r(x,t),\\
\frac{\partial v}{\partial t} &= \frac{\lambda_2 u m}{1+v_2 u} - \frac{\lambda_1 v \eta}{1+v_1 v} + v_r(x,t),\\
\frac{\partial c}{\partial t} &= \frac{\lambda_1 v \eta}{1+v_1 v},\\
\frac{\partial f}{\partial t} &= \beta(f_M - f) f \eta - \frac{\lambda_4 c_a f}{1+v_4 f},\\
\frac{\partial a}{\partial t} &= -\frac{\lambda_3 a \eta}{1+v_3 a} + a_r(x,t),\\
\frac{\partial \iota_a}{\partial t} &= \frac{\lambda_3 a \eta}{1+v_3 a},\\
c_a &= \frac{c}{1+v_e \iota_a}.
\end{aligned} \tag{2.4.13}$$

Again, we remind the reader that in the second mechanism, we have proposed, in which angiostatin itself acts as an inhibitor, the system (2.4.13) simplifies somewhat:

[11] In the literature, $K^i_{cat} = k_{2i}$ and $K^i_m = (k_{2i} + k_{-(2i-1)})/k_{2i-1}$ for $i = 1,\ldots,3$. Thus, $\lambda_i\delta_i = K^i_{cat}/K^i_m$ and $v_i = 1/K^i_m$.

$$\begin{aligned}
\frac{\partial u}{\partial t} &= -\frac{\lambda_2 u m}{1+v_2 u} + u_{\mathrm{r}}(x,t),\\
\frac{\partial v}{\partial t} &= \frac{\lambda_2 u m}{1+v_2 u} - \frac{\lambda_1 v \eta}{1+v_1 v} + v_{\mathrm{r}}(x,t),\\
\frac{\partial c}{\partial t} &= \frac{\lambda_1 v \eta}{1+v_1 v},\\
\frac{\partial f}{\partial t} &= \beta(f_{\mathrm{M}} - f) f \eta - \frac{\lambda_4 c_{\mathrm{a}} f}{1+v_4 f},\\
\frac{\partial a}{\partial t} &= a_{\mathrm{r}}(x,t),\\
c_{\mathrm{a}} &= \frac{c}{1+v_{\mathrm{e}} a}.
\end{aligned} \tag{2.4.14}$$

3. Random walks

Before beginning our discussion of reinforced random walks, we emphasize the issue of time scales once more. Endothelial, pericyte and MCs move at rates that are much smaller than the rates at which the kinetic equations above come to pseudo steady state. That is, time scales for the former movements are of the order L^2/D, whereas the time scales for the latter are $\epsilon = 1/(v_1 k_2 \delta\eta_0) = K_m/(K_{\mathrm{cat}}\delta\eta_0)$. Typically, $L^2/D \approx 100$ days [12] while $\epsilon \approx 50$ s (using the observation that $\delta\eta_0 \approx 1$ μM and data from [13]).

Therefore, in the discussion to follow, we shall assume that the biochemistry of the motion, i.e., the kinetic equations (2.4.5) are already in pseudo steady state, i.e., that Eqs. (2.4.13) are in force at time $t = 0$, the dynamics having been initiated at some time $-\tau < 0$ *but that the endothelial, pericyte and macrophage cells have not yet begun to move*. From now on, time is positive.

In order to describe the dynamics of the endothelial, macrophage and PCs, we employ the ideas of reinforced random walks of [7] as described in [17,18,23]. The primary equation governing the motion of endothelial cells is

$$\frac{\partial \eta}{\partial t} = D_1 \frac{\partial}{\partial x}\left(\eta \frac{\partial}{\partial x}\left(\ln \frac{\eta}{\tau_1}\right)\right), \tag{3.1}$$

where τ_1 is the so-called probability transition function, which in turn depends on one or more of the quantities listed in (2.4.3). [13]

[12] EC movement values here are of the order 10^{-11} cm^2 s^{-1} [28].

[13] Eq. (3.1) can be written in the more standard form

$$\eta_t = D_1 \eta_{xx} - D_1\left(\eta \frac{\partial_c \tau_1 c_x + \partial_f \tau_1 f_x}{\tau_1(c,f)}\right)_x = D_1 \eta_{xx} - D_1(\eta(\ln \tau_1)_x)_x, \tag{3.2}$$

which may be a form more familiar to some readers. However, if one thinks of (3.1) as a diffusion process for a reinforced random walk, then the long time tendency for such a process will be to drive η in such a way as to bring the ratio η/τ_1 to unity. In other words, the 'walker density equation' asserts that the walker will move in such a way as to have a large probability density where the probability transition rate is large and a small probability density where it is small.

In this case, we regard the motion of endothelial cells to be influenced by the active part of the proteolytic enzyme it produces (C_A) and by the proteins such as fibronectin in the BL, i.e., we write

$$\tau_1 = \tau_1(c_a, f). \tag{3.3}$$

A simple transition probability which reflects the influence of enzyme and fibronectin on the motion of endothelial cells is $\tau_1(c_a, f) = c_a^{\gamma_1} f^{-\gamma_2}$ for positive constants γ_i. The probabilistic interpretation of this choice is that endothelial cells prefer to move into regions where c_a is large or where f is degraded, facts which have basis in biological experiment.

Remark 4. Since (3.1) is derived as the continuous limit of a reinforced random walk, [23], the transition probability τ_1 provides the link between microscopic and macroscopic events. As a consequence, the selection of an appropriate choice for τ_1 represents a challenging problem in cell biology and biochemistry. Our choice for τ_1 is therefore phenomenological. That is, *it reflects the known facts that EC cell movement depends not only upon protease and fibronectin gradients but also upon their concentration.*

For example, it is known [5] that EC will tend to aggregate at density levels of fibronectin which are around 25% of maximal concentrations of fibronectin. In other words, EC cell movement depends not only on gradients in fibronectin but also upon its density.

Moreover, if there is too little protease present endothelial cells cannot invade a tissue. On the other hand, if protease is in excess, the enzyme will even attack the proteins in the cell surface and eventually destroy the cell itself. This too suggests that sensitivity factors depend not only upon the gradient of active protease but also upon its concentration.

Remark 5. If we adopt a more classical viewpoint in which ECs are presumed to respond solely to the gradients in c_a and f, then we would take

$$\tau_1(c_a, f) = \exp(\chi c_a + \rho f), \tag{3.4}$$

where χ is the chemotactic coefficient and ρ is the haptotactic coefficient.

However, with this choice of τ_1, the sensitivity coefficients, $\partial_{c_a}\tau_1/\tau_1$ and $\partial_f\tau_1/\tau_1$, which determine the 'drift' in (3.1) are not dependent on the concentrations of c_a and f.

This choice, however, is at variance with the biological evidence as discussed above.

These facts, together with our prior experience with related equations in [17] motivated our choice for τ_1. There, we found that it was not so much the gradient in the concentration of the chemotactic agent that was significant in determining aggregation or deaggregation of particles which move chemotactically under reinforced random wall but rather the *relative gradient* i.e., the gradient of the logarithm of the concentration, which played a significant role in the aggregation of the particles.

We adopt this viewpoint in the choice of subsequent probability transition factors.

In order to avoid singularities in $\ln\tau_1$ and its derivatives in (3.1), it is useful to take

$$\tau_1(c_a, f) = \left(\frac{c_a + \alpha_1}{c_a + \alpha_2}\right)^{\gamma_1} \left(\frac{f + \beta_1}{f + \beta_2}\right)^{\gamma_2}, \tag{3.5}$$

where the α_i, β_i are empirical constants such that $0 < \alpha_1 \ll 1 < \alpha_2$ and $\beta_1 > 1 \gg \beta_2 > 0$. Clearly then, (3.5) is not singular for small or large values of c_a, f and will approximate $c_a^{\gamma_1} f^{-\gamma_2}$ reasonably well over a considerable range of these variables.

This choice allows us to 'control' the distribution of endothelial cells in the opening of the forming sprout. Basically, the observation to be made is that the larger $|\alpha_2 - \alpha_1|\gamma_1 + |\beta_2 - \beta_1|\gamma_2$ is, the more bimodal this distribution is in the opening channel. (In the extreme case that this sum is zero, the cells do not move at all *in response to gradients in fibronectin or in protease*.) On the other hand, when we are in the simple power law case, we may have single point or even double point blow up. That single point blow up occurs was rigorously demonstrated in the simpler case of one sensitivity factor in [17]. (A theoretical rationale for when single point or double point blow up may be expected to occur is given in the next section.)

The PC density σ is taken to satisfy

$$\frac{\partial \sigma}{\partial t} = D_2 \frac{\partial}{\partial x}\left(\sigma \frac{\partial}{\partial x}\left(\ln \frac{\sigma}{\tau_2}\right)\right). \tag{3.6}$$

To model the decrease in pericyte population in regions where the fibronectin is low, we assume that the pericyte density is large where the fibronectin density is large and small where the latter is small. To make this precise in the context and language of the random walk mechanism, we may think of fibronectin as a chemotactic attractant for PCs. We take

$$\tau_2(f) = \left(\frac{f + \alpha_3}{f + \alpha_4}\right)^{\gamma_3}, \tag{3.7}$$

where $0 < \alpha_3 \ll 1 \ll \alpha_4$.

Finally, the MC density $m(x,t)$ is assumed to satisfy

$$\frac{\partial m}{\partial t} = D_3 \frac{\partial}{\partial x}\left(m \frac{\partial}{\partial x}\left(\ln \frac{m}{\tau_3}\right)\right), \tag{3.8}$$

where we expect that the MCs will be attracted to the pathological agents in the body, in this case, the chemotaxic agent. Thus, it is reasonable to write

$$\tau_3(u) = \left(\frac{u + \beta_3}{u + \beta_4}\right)^{\gamma_4}, \tag{3.9}$$

where $0 < \beta_3 \ll 1 \ll \beta_4$.

The system (2.4.11) with (3.1)–(3.9) (or (2.4.12) with (3.1)–(3.9) is closed by imposing the no flux boundary conditions

$$\eta \frac{\partial}{\partial x}\left(\ln \frac{\eta}{\tau_1}\right) = \sigma \frac{\partial}{\partial x}\left(\ln \frac{\sigma}{\tau_2}\right) = m \frac{\partial}{\partial x}\left(ln \frac{m}{\tau_3}\right) = 0 \tag{3.10}$$

at $x = 0, L$.

The initial conditions for the system (2.4.11) with (3.1)–(3.9) are

$$\begin{aligned} &\eta(x,0) = \eta_e, \quad \sigma(x,0) = \sigma_e, \quad m(x,0) = m_e, \\ &u(x,0) = 0, \quad v(x,0) = 0, \quad c(x,0) = 0, \\ &a(x,0) = 0, \quad \iota_a(x,0) = 0, \quad f(x,0) = f_M, \end{aligned} \tag{3.11}$$

where $\eta_e, \sigma_e,$ and m_e are the (constant) cell densities along the capillary axis and f_M is the density of fibronectin in the capillary wall. (In the case of system (2.4.12) with (3.1)–(3.8), the initial condition for ι_a is omitted from (3.11).)

In order to initiate the dynamics, we assume that the tumor supplies angiogenic factor or chemotactic factor at rates u_r, v_r as discussed in Remark 3. In order to test the efficacy of our 'treatment', we may introduce an angiostatic agent at a given rate $a_r(x,t)$ as also discussed in Remark 3.

4. Elements of theoretical analysis

A complete stability analysis of (2.4.13), (3.1)–(3.8) (or the simplified system) together with (3.10) and (3.11) when there are no forcing terms ($u_r = v_r = a_r \equiv 0$) would take us far beyond the scope of the current paper.

For example, if we renormalize η, σ, m, f by replacing them by $\eta/\eta_e, \sigma/\sigma_e, m/m_e, f/f_M$, then the nine-tuple $(\eta, \sigma, m, u, v, c, a, \iota_a, f)$ will be a stationary solution of the resulting system when it is of the form $(1,1,1,0,0,0,0,0,1)$. [14] Likewise, another stationary point is $(1,1,1,0,0,0,0,0,0)$. (This renormalization will induce a corresponding rescaling in the probability transition function constants, the rate constants, λ_i and the fibronectin production constant, β.)

In order to test the stability of each of these solutions, one would have to perturb each component and then write down the linearized equations relative to the perturbation. However, since this system is not of standard parabolic type (in particular, it is strongly coupled), no suitable stability theory exists for it at present.

There are three genuine partial differential equations (in η, σ and m), which are parabolic in these variables and hence these variables possess the infinite speed of propagation principle. On the other hand, the remaining equations are ordinary differential equations in the remaining variables and consequently these variables possess zero propagation speed.

As explained in [17,18,23] (for somewhat simpler systems), this means that several possibilities can occur for the cell density functions when one perturbs the stationary solution. These are: (i) finite time blow up, (ii) growth and subsequent collapse to the constant initial value and (iii) aggregation to a spatially non-constant solution.

Perhaps the best way to understand this system is to consider the special case in which the sensitivity factors (the $\tau's$) are all power laws and then show how the system has substructures reminiscent of the system considered in [17,18,23].

To do this, we take $a(x,0) = 0 = a_r(x,t)$ so that $c(x,t) \equiv c_a(x,t)$. That is, we consider the problem without angiostatin. Then, both models that include angiostatin reduce, mathematically, to the same set of partial differential equations.

(It is not to hard to see from an intuitive examination of the two systems with angiostatin that if $c_a \to 0$ as $t \to +\infty$, then $f \to 1$ and the cell densities η, σ should converge to constants. If a_r is strictly positive, then we might expect that $c_a \to 0$. If $a(x,0) > 0$, then we expect that there will be a tendency for the active enzyme density to converge to zero, at least for a short time.)

[14] Notice that when $c = 0$, $c_a = 0$ also.

Set $\tau_1(c,f) = c^{\gamma_1} f^{-\gamma_2}$, $\tau_2(f) = f^{\gamma_3}$ and $\tau_3(u) = u^{\gamma_4}$. Then, the simplified version of our system which should capture the essential features of our numerical results when no angiostatic agent is present, takes the form

$$\begin{aligned}
\eta_t &= D_1\eta_{xx} - D_1\left[\eta\left(\gamma_1\frac{c_x}{c} - \gamma_2\frac{f_x}{f}\right)\right]_x,\\
\sigma_t &= D_2\sigma_{xx} - D_2\left[\sigma\left(\gamma_3\frac{f_x}{f}\right)\right]_x,\\
m_t &= D_3 m_{xx} - D_3\left[m\left(\gamma_4\frac{u_x}{u}\right)\right]_x
\end{aligned} \tag{4.1}$$

for the cell motion equations, while the relevant chemical transport equations are

$$\begin{aligned}
\frac{\partial u}{\partial t} &= -\lambda_2 um,\\
\frac{\partial v}{\partial t} &= \lambda_2 um - \lambda_1 v\eta,\\
\frac{\partial c}{\partial t} &= \lambda_1 v\eta,\\
\frac{\partial f}{\partial t} &= \beta f\eta - \lambda_4 cf,
\end{aligned} \tag{4.2}$$

where we are assuming that $v_4 f \ll 1$. Throughout this section we take $L = 1$ for convenience.

Our assertion here is that any instabilities in the full system arise from positive perturbations of the stationary solution $(\eta,\sigma,m,u,v,c,f) = (1,1,1,0,0,0,0)$. The system (4.1) and (4.2) can then be thought of as the linearization of the full system (without angiostatic agent) about this solution. (Of course one has to interpret the ratios $u_x/u, c_x/c, f_x/f$ with some care in this context.)

Notice that $u(x,t) + v(x,t) + c(x,t) = u(x,0) + v(x,0) + c(x,0)$. We want to drive our system from an initial perturbation of $u(x,0) = 0$. We take $(u(x,0), v(x,0), c(x,0)) = (\theta_0(x), 0, 0)$, where θ_0 is a small, positive, non-constant, unimodal function, for example, $\delta(1 - \epsilon\cos(2\pi x))^m$ with δ small and positive. Now u is always decreasing in t, while v initially increases in t. As u is consumed, v eventually decreases in t and is thus bounded (for each x for which $\eta(x,\cdot)$ and $m(x,\cdot)$ are bounded and bounded away from zero). Consequently, c is always strictly increasing in t whenever $v\eta > 0$ and is always non-decreasing. (The variables (η,σ,m,u,v,c,f) are always assumed to be non-negative.)

The conservation law tells us that $c(x,t) \leqslant u(x,0) + v(x,0) + c(x,0)$. Thus, c increases to some limit function $\theta(x) > 0$, where $\theta \leqslant \theta_0$. [15]

[15] If we knew that $u, v \to 0$ as $t \to +\infty$, then we could take $\theta(x) \equiv \theta_0(x)$. This will be the case for u if $m(x,\cdot)$ is bounded away from zero since then u will decay exponentially fast as we see using an argument similar to that following (2.4.11). A similar argument shows that if u decays exponentially fast and if $\eta(x,\cdot)$ is bounded away from zero then v also decays exponentially fast.

We consider the critical point $(1,1,1,0,0,0,0)$. The subsystem of (4.1) and (4.2) of interest is

$$\begin{aligned}\frac{\partial \eta}{\partial t} &= D_1\eta_{xx} - D_1\left[\eta\left(\gamma_1\frac{\theta_x}{\theta} - \gamma_2\frac{f_x}{f}\right)\right]_x,\\ \frac{\partial f}{\partial t} &= \beta f\eta - \lambda_4\theta f.\end{aligned} \tag{4.3}$$

This system was discussed in [18], where it was shown that if we make the change of variables $g = \ln f$, we are led to

$$\mathscr{L}g \equiv g_{tt} - D_1\gamma_2(g_tg_x)_x = D_1g_{xxt} + G(g_x, g_t, \theta, \theta', \theta''). \tag{4.4}$$

Inspection of the function G, reveals that it is linear in ∇g and vanishes as $\theta, \theta'/\theta, \theta'' \to 0$. The second order, quasi-linear operator $\mathscr{L}$ has discriminant

$$\mathscr{D}(x,t) \equiv \mathscr{D}(g_x(x,t), g_t(x,t)) = D_1\gamma_2(D_1\gamma_2g_x^2 + 4g_t). \tag{4.5}$$

The operator $\mathscr{L}$ will therefore be elliptic in those regions, where $\eta < \lambda_4\theta(x)/\beta$ ($g_t < 0$) and where $\mathscr{D}(x,t) < 0$, i.e., where η is small and f is small and nearly constant (so that $g_x = f_x/f \approx 0$). On the other hand, if $\mathscr{D}(x,t) > 0$, then the operator will be hyperbolic. This will occur if $\eta > \lambda_4\theta/\beta$. The numerical observation of Levine and Sleeman [17], which was also supported by the properties of an exact solution of

$$g_{tt} - D_1\gamma_2(g_tg_x)_x = D_1g_{xxt} \tag{4.6}$$

was that single point blow up of (4.6) occurs on the parabolic boundary of the operator $\mathscr{L}$ and hence should occur on the parabolic boundary of (4.4). Suppose for (4.4) we take $g(x,0) = -a^2$ for some constant $a > 0$ (corresponding to a small positive constant perturbation of $f(x,0) = 0$) and $\eta(x,0) = 1$. Then, $g_t(x,0) = \beta\eta_e - \lambda_4\theta_0 = \beta - \lambda_4\delta(1 - \epsilon\cos(2\pi x))^m$. Assume also that

$$(1-\epsilon)^m < \frac{\beta}{\delta\lambda_4} < (1+\epsilon)^m,$$

which can always be arranged for fixed $\delta, \epsilon \in (0.1)$ if $m \gg 1$. Consequently

$$\mathscr{D}(x,0) = 4D_1\gamma_2g_t(x,0)$$

and has exactly two sign changes, being negative near $x = 1/2$ and positive near $x = 0, 1$. Thus, two parabolic curves evolve from the two points for which $\mathscr{D}(x,0) = 0$. Consequently, we expect that the solutions of (4.6) (and likewise of (4.4)) to blow up in finite time along these curves.

Next suppose that we perturb the stationary point $(1,1,1,0,0,0,1)$. We take the perturbation in the form $(u(x,0), v(x,0), c(x,0)) = (0,0,\theta_0(x))$, where $\theta_0(x) \equiv \delta(1 - \epsilon\cos(2\pi x))^m$. The actual form of the rate law for f_t assures us that $f \leqslant 1$. We see from the full differential equation that near $t = 0$ $f_t \approx -\lambda_4\theta_0(x)f$ since $f \approx 1$ near $t = 0$. This obviously tells us that protease will initiate degradation of the capillary wall. More than this, however, it tells us that we may expect the width of the opening to be closely correlated to the power m in θ_0. (The larger m is, the narrower should be the opening of the nascent capillary.) We illustrate this in some of the numerical computations.

We suggest that these two observations form the underlying mechanism for the bimodal structure observed in the endothelial cell density computations given in the next section.

Consider next, the subsystem:

$$\begin{aligned} m_t &= D_3 m_{xx} - D_3\left[m\left(\gamma_4 \frac{u_x}{u}\right)\right]_x, \\ \frac{\partial u}{\partial t} &= -\lambda_2 u m. \end{aligned} \tag{4.7}$$

If we take $\psi = -\ln u$, then we find that

$$\psi_{tt} + D_3\gamma_4(\psi_t\psi_x)_x = D_3\psi_{xxt}. \tag{4.8}$$

This is precisely the equation studied in [17,23] with $\psi(x,0) = 0$ and $\psi_t(x,0) = (1 - \epsilon\cos(2\pi x))$. It was shown numerically in [23] that when $m = 1$ solutions appeared to blow up in finite time. In [17], exact solutions were found which blew up in finite time. [16] The singularity formed precisely on the parabolic boundary as remarked above.

With $m(x,0) = 1$ and $u(x,0)$ again a small multiple of $(1 - \epsilon\cos(2\pi x))^m$ (for small positive ϵ so that $\ln u(x,0)$ is well defined) and no flux boundary conditions, we again have

$$\mathscr{D}(x,0) = 4\gamma_4 D_3\left(\frac{\gamma_4 D_3 m^2\epsilon^2\sin^2(2x)}{(1-\epsilon\cos(2x))^2} - 1\right).$$

Indeed, it is negative at the center and ends of the interval and will be positive at $x = \pi/4$ and $3\pi/4$ if $m^2\epsilon^2 D_3\gamma_4 > 1$. This means that our solution will initially be partially in the elliptic region and partially in the hyperbolic region. We then expect single point blow up on each of the two curves emanating from the x-axis for which $\mathscr{D}(x,t) = 0$ which form the boundary of the central elliptic region. See [18] (Section 6) for an illustrative computation. Likewise, then, we expect the behavior of MC densities which are observed numerically in the figures.

The behavior of the PC density solution can be understood neglecting 'cell diffusion' in the second of (4.1) and considering instead the hyperbolic initial value problem

$$\begin{aligned} &\sigma_t = -D_2\left[\sigma\left(\gamma_3\frac{f_x}{f}\right)_x\right]_x \quad \text{for} \quad -\infty < x < \infty, \\ &\sigma(x,0) = 1, \end{aligned} \tag{4.9}$$

where $f(x,t)$ is regarded as a known function. In particular, if we take $f(x,t) = F(x)$ where $F(x) = 1 - \epsilon e^{-\lambda x^2}$, then the behavior of the solution σ of (4.9) is the following: first, σ will be an even function of x; secondly, for $x_0 > 0$ the characteristic given by $x(x_0,t)$ starting at x_0 will increase with time. Finally, along this characteristic, $\sigma(x(x_0,t),t)$, will be an increasing function of t. Thus, we can expect σ to aggregate near the maxima of f and collapse near the minima of f. This was also observed for the full problem in the computations below.

5. Numerical experiments

In this section we consider some computations based on the initial-boundary value problem for the above system. (That is, we solve numerically, the system consisting of (2.4.13), (3.1)–(3.8)

[16] The initial data for the exact solution agreed with the above initial data in the limit as $\epsilon \to 0$.

together with (3.10) and (3.11) using the τ_i as discussed above.) In order to keep the number of figures to a manageable level, we consider only three cases. In the first case no angiostatin is present. In the remaining cases, angiostatin either functions directly as an inhibitor or else as a substrate which is transformed into an inhibitor via the receptor mechanism we discussed earlier.

In all cases, we assume that the initial concentrations of the chemical species; the chemotactic agent, K, the angiogenic factor (TAF), the proteolytic enzyme, the inhibitor and the angiostatic agent are all zero as discussed above.

We also assume that $v_r(x,t) = 0$ in order to test the mechanism for the production of proteolytic enzyme from chemotactic factor through the entire chemical mechanism without interference from tumor-generated angiogenic factor.

We assume that the tumor produces a chemotactic agent at a rate $u_r(x,t)$ given by

$$u_r(x,t) = u_0\kappa_m[(1-\cos(2\pi x))]^m e^{-\theta t}. \tag{5.1}$$

The assumption here is that in the avascular state, the tumor emits a chemotactic agent at a rate which will decay with time. The constant m is to be thought of as a measure of how 'concentrated' or localized the angiogenic factor is. That is, the sequence of functions $F_m(x) \equiv \kappa_m[1-\cos(2\pi x)]^m$ forms a δ sequence. [17] The decay rate, θ can be thought of as a measure of the survivability of the tumor in the avascular state. (Here k_m is a normalizing constant taken to ensure that

$$\int_0^1 u_r(x,t)\,dx = u_0\exp(-\theta t)$$

and consequently

$$\int_0^\infty \int_0^1 u_r(x,t)\,dx\,dt = \frac{u_0}{\theta}.$$

That is, θ is inversely proportional to the total quantity of chemotactic agent supplied by the tumor.) In the worst case, when $\theta = 0$, the total rate of supply of chemotactic factor is u_0 at the capillary and is constant in time.

In the first case, we take $a_r(x,t) = 0$, so that there is no angiostatic agent being present in the capillary to mitigate the effects of the proteolytic enzyme on the fibronectin.

In the second case, we consider what happens when we introduce the angiostatic agent at a uniform rate $a(x,t) = A_0$. $a_r(x,t)$ to be a positive constant (see Remark 3).

In a real system, $\theta > 0$. However, to test the model and the effect of angiostatic agent we take $\theta = 0$ as a worst case situation.

We have carried out computations without angiostatin and for the two models for the action of angostatin. In the case for which angiostatin induces EC production of inhibitor, there are ten dependent variables ($\eta, \sigma, m, u, v, a, c, c_a, \iota_a$ and f). Thus, to present all of our computations we would have to present 20 figures (10 without the angiostatic agent, and 10 with the angiostatic agent). However, the biological variables that can be observed directly in sections of tissue under the microscope, at least in principle, are just the three cell species and the thickness of the basal

[17] We have $\lim_{m\to+\infty} F_m(x) = \delta(x-(1/2))$, the δ function concentrated at $x = 1/2$, in the sense of distributions.

lamina. Therefore, we only present plots of the variables $\eta, \sigma, m,$ and f in each of the two cases. This reduces the total number of figures to 12 (four for the case of now angiostatin, four for the case in which angiostatin produces and inhibitor and four where it acts as an inhibitor).

Remark 6. The issue of how to renormalize the system of equations listed above in an efficient way is not a trivial one. Basically there are two ways to proceed:

1. We could rescale each of the variables $\eta, \sigma, m, u, v, a, c, c_a, \iota_a$ and f by dividing each of them by their corresponding values in a normal capillary, say $\eta_e, \sigma_e, m_e, u_e, v_e, a_e, c_e, c_{ae}, \iota_{ae}$ and f_e. [18] One difficulty with this procedure is that while there are small amounts of growth factors, protease, growth factors and angiostatins present in normal tissues, literature values for these background values are hard to come by or are not known. [19]
2. An alternate way to proceed is to renormalize the cell densities and fibronectin as described above. One can then renormalize u, v, c, a, ι by replacing them by ratios $u/u_0, v/v_0, c/c_0, a/a_0, \iota/\iota_0$ where the values $u_0, v_0, c_0, a_0, \iota_0$ are found from experiment in the stroma surrounding a malignant tumor. (This is what was done for a much simpler model in [2] for example.) However, here again the search for such values in the literature provides little information although data are available for v_0 [2].

In this paper, we have taken a hybrid approach. We have rescaled the cell densities to unity since the cell transport equations are linear in them. (This we cannot do in the more complex model in [16], since then mitosis in the ECM must be included in the two-dimensional model.) However, we have not rescaled the concentrations for the chemotactic agent nor for the growth factor, the inhibitor or the angiostatic agent. Rather, we assume that their concentrations are given in μM (micromoles per liter). This allows us to directly insert literature values for the λ_i, ν_i (when expressed in terms of K_{cat}, K_m in units of reciprocal hours and micromoles, respectively) directly into our programs.

These observations lead us to write, for our initial conditions for the angiostatin–inhibitor system:

$$\begin{aligned} &\eta(x,0) = 1, \quad \sigma(x,0) = 1, \quad m(x,0) = 1, \\ &u(x,0) = 0, \quad v(x,0) = 0, \quad c(x,0) = 0, \\ &a(x,0) = 0, \quad \iota_a(x,0) = 0, \quad f(x,0) = 1, \end{aligned} \tag{5.2}$$

where we have normalized the cell densities and fibronectin density to be unity at the outset. Since the cell movement equations are linear in the cell densities, we can carry out this rescaling without affecting the constants in the η, σ, m dynamical equations. As a consequence, this will involve

[18] The background values $v_e, a_e, c_{ae}, \iota_{ae}$ are the concentrations of the variables in normal tissues that balance the tendency for angiogenesis to occur with the tendency for the body to inhibit it [11].

[19] A second difficulty with this approach is that we must then incorporate into our model production terms $\sigma_1\eta$ and $\sigma_2\eta$ in the rate equations for TAF and for angiostatin (because endothelial cells are known to produce both types of molecules) and decay terms $-\mu c$ and $-\mu'\iota$ since it is also well known that protease and inhibitors decay. This would further complicate our model. It would also make our search for decay constants much more problematic since while there are literature values for some of these compounds, they have been found only from in vitro experiments.

Table 1
Data set for numerical simulations (units are given in the discussion following remark 7)

$\eta(x,t)$ (Endothelial cell movement)	$D_1 = 3.6 \times 10^{-5}$	$\alpha_1 = 0.001$	$\alpha_2 = 1.0$	$\gamma_1 = 1.2$
η (EC movement continued)		$\beta_1 = 1.0$	$\beta_2 = 0.001$	$\gamma_2 = 1.2$
$\sigma(x,t)$ (PC movement)	$D_2 = 3.6 \times 10^{-5}$	$\alpha_3 = 1.5 \times 10^{-3}$	$\alpha_4 = 1.0$	$\gamma_3 = 2.0$
$m(x,t)$ (MC movement)	$D_3 = 3.6 \times 10^{-5}$	$\beta_3 = 0.5$	$\beta_4 = 1.0$	$\gamma_4 = 2.0$
u (Chemotactic factor kinetics)	$\lambda_2 = 75.0$	$\nu_2 = 0.01$		
v (Angiogenic factor kinetics)	$\lambda_1 = 73.0$	$\nu_1 = 0.007$	$\nu_r(x,t) = 0.0$	
c (Proteolytic enzyme kinetics)	$\lambda_1 = 73.0$	$\nu_1 = 0.007$	$\mu = 0.0$	
f (Fibronectin rate law)	$\beta = 0.22$	$\lambda_4 = 19.0$	$\nu_4 = 1.205$	$f_m = 0.01$
$a, \imath_a$(Angiostin as inhibitor generator)	$\lambda_3 = 100.0$	$\nu_3 = 0.002$	$\nu_e = 1.0 \times 10^3$	
a_r (Angiostatin as inhibitor generator)	$a_r(x,t) = 0.0$	$a_r(x,t) = 25.0$		
a_r (Angiostatin as inhibitor)		$a_r(x,t) = 250.0$	$\nu_e = 1.00$	
u_r (Chemotactic factor forcing term)		$u_0 = 15$	$\theta = 0.0$	$m = 40$

redefinition of the constants λ_i as $\lambda_1\eta_e, \lambda_2 m_e, \lambda_3\eta_e$ in the ordinary differential equations for $u, v, c, f, a, \imath$ and as λ_4, f_M in the fibronectin production equation. This choice also allows us to insert the literature values of K_{cat}, K_m directly into the model equations without rescaling. In the literature, these values have units of h^{-1} and μM, respectively.

Remark 7. Taken together, there are 33 constants to be retrieved from the literature. Many of the values we are using have been found by John Henrichsen using Pub Med, [20] a search engine designed especially for searches of the medical bioscience literature.

We use the constants given in Table 1.

Length will be expressed in millimeters unless otherwise specified. Time will be expressed in hours. Concentrations and densities will be in micromolarity, i.e., in micromoles per unit liter to conform to the biological literature.

The sensitivity parameters, $\alpha_i, \beta_i, \gamma_i$ were chosen for illustrative purposes only; we took $L = 50$ μm $= 0.05$ mm. They must be determined experimentally and this has yet to be done. The units for the α_i, β_i will be in micromoles per liter.

Since, we know that the average capillary diameter is about 10 μm or 0.01 mm in diameter, the scale we have chosen is such that x is expressed in tenths of millimeters. Experimentation with the power m in u_r indicates that when $m = 40$, the opening in fibronectin will be about 0.01 mm. (See the comments in Section 4.)

The cell movement constants above are of order of magnitude found in [28], when expressed in units of $mm^2\ h^{-1}$. For example, $10^{-10}\ cm^2\ s^{-1} = 3.6 \times 10^{-7}\ cm^2\ h^{-1} = 3.6 \times 10^{-5}\ mm^2\ h^{-1}$.

The values taken from [13] for the VEGF receptor KDR tyrosine kinase yield $\lambda_1 = K_{cat}/K_m \approx 162 \times 60/130 \approx 73$ per μM per hour and $K_m \approx 130$ μM. This gives a corresponding value for $\nu_1 \approx 0.007\ (\mu M)^{-1}$.

[20] http://www.ncbi.nlm.nih.gov/pubmed

Literature values for the chemotactic factor (λ_2, v_2) have not yet been found. The values we took are of the same order of magnitude as those for the growth factor.

For 'fibronectin', we have taken values for λ_4, v_4 from [9]. We took, $K_{\text{cat}} = 16$ per hour and $K_m = 0.83$ μM for the hydrolysis of type I collagen (rat tendon). by human fibroblast collagenase (HFC).

The constant β is estimated as follows. We know that in $T = 18$ h, f_{M} moles of fibronectin will be generated by η_0 endothelial cells. [33,22]. In th absence of protease, we have $f_t = \beta_1 f(f_{\text{M}} - f)\eta_0$ so that, very nearly, we can write $f_{\text{M}}/T \approx \beta_1 \eta_0 f_{\text{M}}^2 x(1-x)$, where $x = f/f_{\text{M}}$. The maximum value of $x(1-x)$ on $[0,1]$ is 0.25. This gives a maximum possible value $\beta_1 \approx 4/(Tf_{\text{M}}\eta_0)$. Renormalizing the equation $f_t = \beta_1 f(f_{\text{M}} - f)\eta - c_{\text{a}}\lambda_4 f/(1 + v_4 f_{\text{a}})$ so that $\eta_0 = 1$ and $f_{\text{M}} = 1$, we have $\beta = \beta_1 \eta_0 f_{\text{M}} = 4/T \approx 0.22\ \text{h}^{-1}$. We must also replace v_4 by $v_4 f_M$. From [31] we estimate f_M as approximately 10^{-2} μM.

The protease inhibitor equilibrium constants (dissociation constant) (v_{e}) tend to be very large. For example, the value $v_{\text{e}} \approx 1000\ (\mu\text{M})^{-1}$ is taken from [32] and was for the inhibition of phosphorylated urokinase-type plasminogen activator (P-uPA) by inhibitor PAI-1.

A search of the Pub Med data base for angiostatin – receptor kinetic parameters (K_{cat}, K_m) suggests that there is not yet experimental evidence for the mechanism proposed here in which angiostatin stimulates the production of protease inhibitor. Therefore, in the absence of other information, it seems reasonable to take these numbers to be of the same order of magnitude as

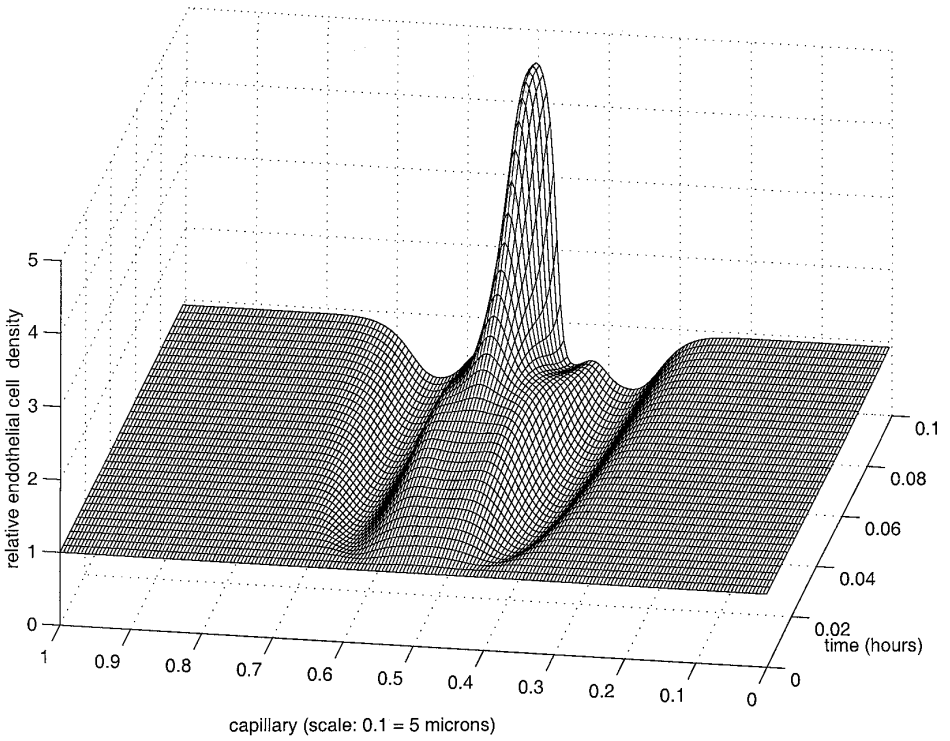

Fig. 6. Time course for endothelial cell density, $\eta(x,t)$, no angiostatin ($t = 0.1$ h).

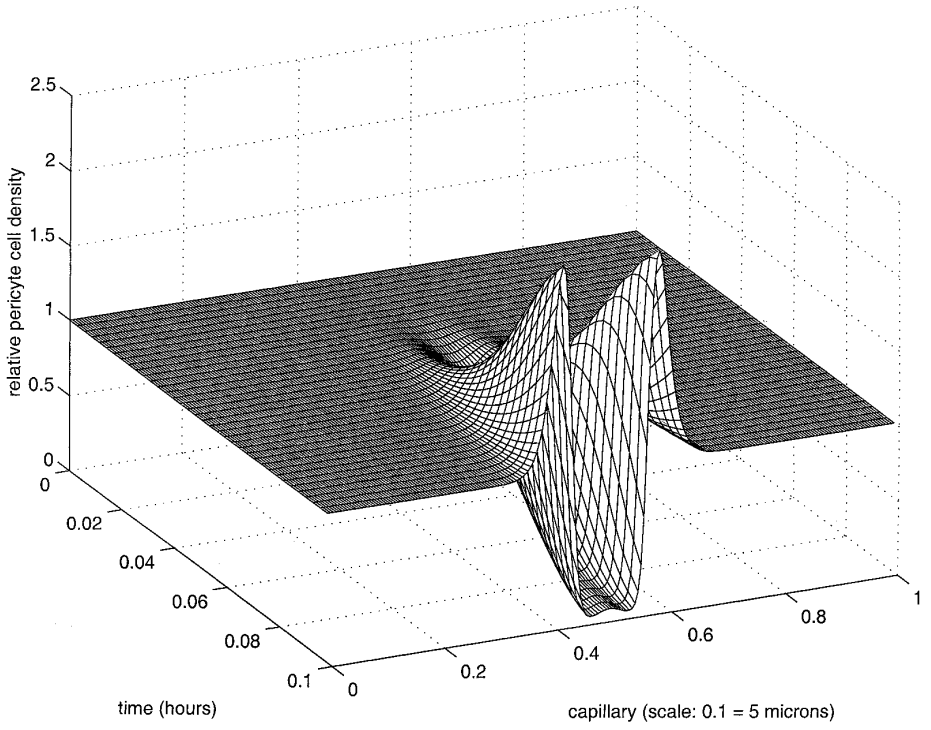

Fig. 7. Time course for PC density, $\sigma(x,t)$, no angiostatin ($t = 0.1$ h).

those for the chemotactic agent and the growth factor since the assumption is that the angiostatin interacts with cell receptors in the same manner as do the former two agents.

However, it is has been demonstrated that angiostatin derived from plasminogen itself inhibits the action of tPA. When angiostatin acts directly as an inhibitor of the protease, an equilibrium constant $v_e \approx 1$ μM was reported in [27].

It is perhaps worth emphasizing that the constants a_r, u_0 in the above table have the units of micromolarity per hour. In the actual program we took

$$a_r(x,t) = a_0 H(t - t_0),$$

where t_0 is a waiting time to begin therapy and where a_0 is one of the dosage rates (a_r) listed in the table above. [21]

The obvious conclusion, that the sooner one begins the therapy (that is, the smaller t_0 is), the more quickly and effaciously is the degradation caused by the chemotactic agent undone. In the simulations we took $t_0 = 0.0$.

In order to compare the mechanisms for angiostatin, we took $a_r = 25$ μM h^{-1} for the angiostatin–inhibitor system and $a_r = 250$ μM h^{-1} for the angiostatin as inhibitor system. The dosage rate is larger in the second case because the equilibrium constant (v_e) is smaller.

[21] Here $H(x)$ is the Heaviside step function, $H(x) = 1$ if $x > 0$, and $H(x) = 0$ otherwise.

6. Remarks on computations

Computations with systems of equations such as these are very sensitive to step size ratios. Furthermore, as in all numerical computations, decreasing step size is not a guarantee of convergence to the true solution as round off error will ultimately defeat this procedure. In the computations we present below, we proceeded along these lines with various $D\delta t/(\delta x)^2$ ratios, which satisfied the CFL condition until round off error interfered. The figures in the no-angiostatin cases were generated as far out in time as the numerical scheme would permit for various ratios.

7. Conclusions and discussion

A careful examination of Figs. 6–18 allows us to draw some conclusions based on the computations.

In Figs. 6–9, we have plotted the time course of the system without angiostatin present. We note in Figs. 6–8, the formation of unimodal cell distributions in endothelial cell and macrophage cell distributions as time evolves which persist until numerical instability sets in. On the other hand, the pericyte cell distribution becomes bimodal. The choice of u_0 affects these distributions. In

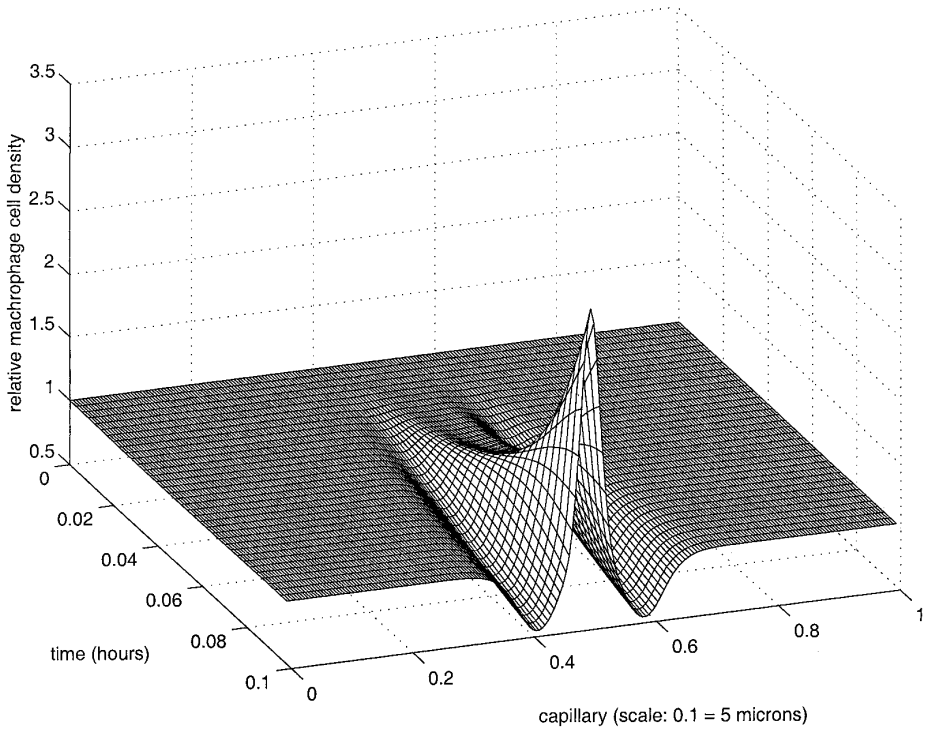

Fig. 8. Time course for macrophage density, $m(x,t)$, no angiostatin ($t = 0.1$ h).

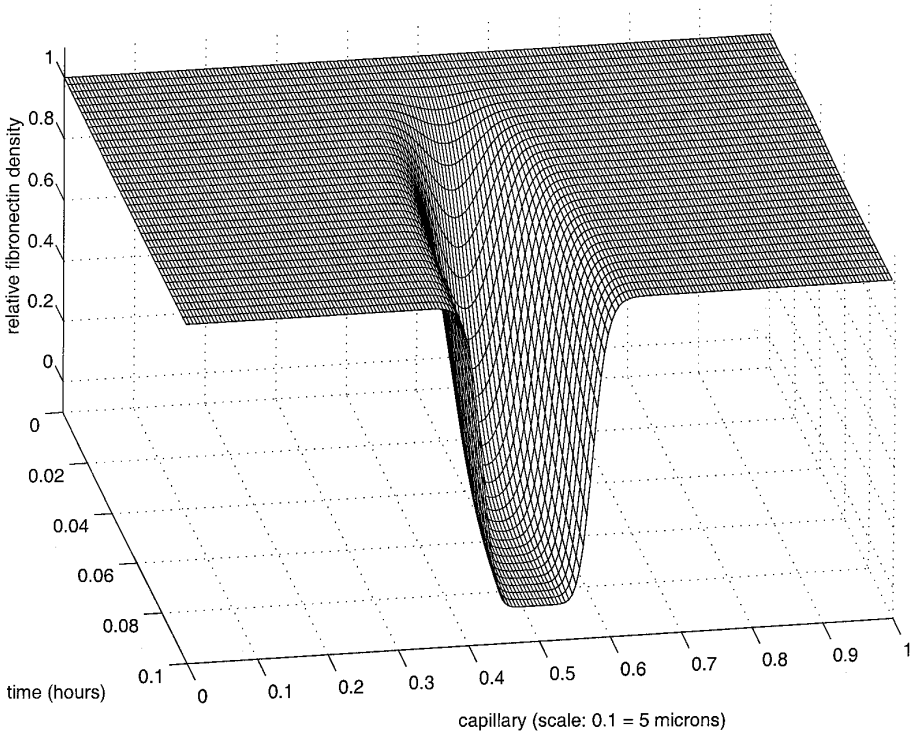

Fig. 9. Time course for fibronectin density, $f(x,t)$, no angiostatin ($t = 0.1$ h).

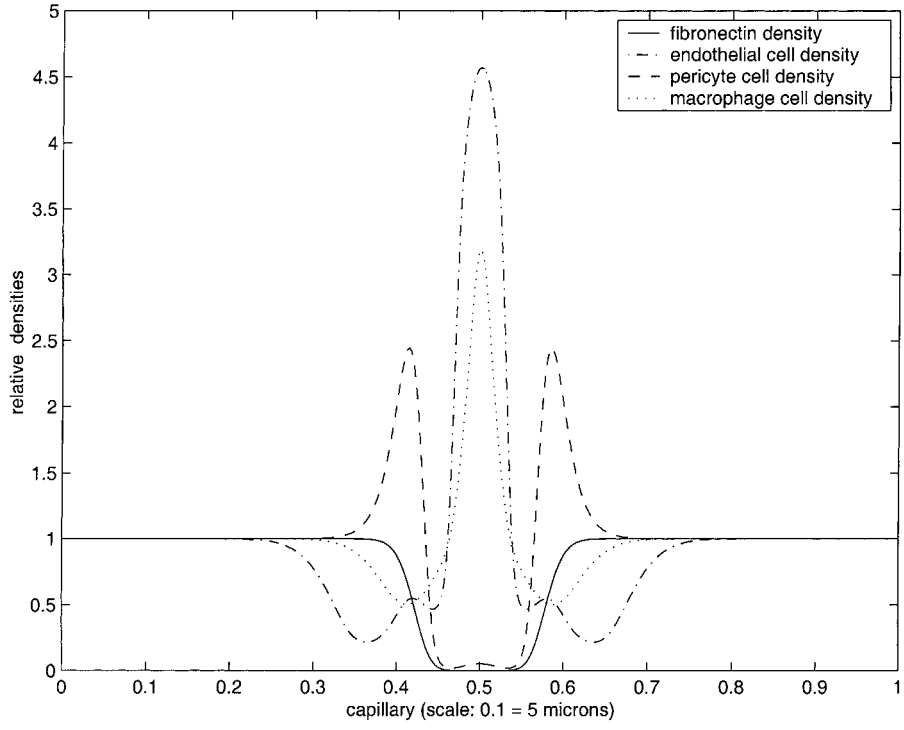

Fig. 10. Final time profiles of comparative cell and fibronectin densities in the absence of angiostatic agent.

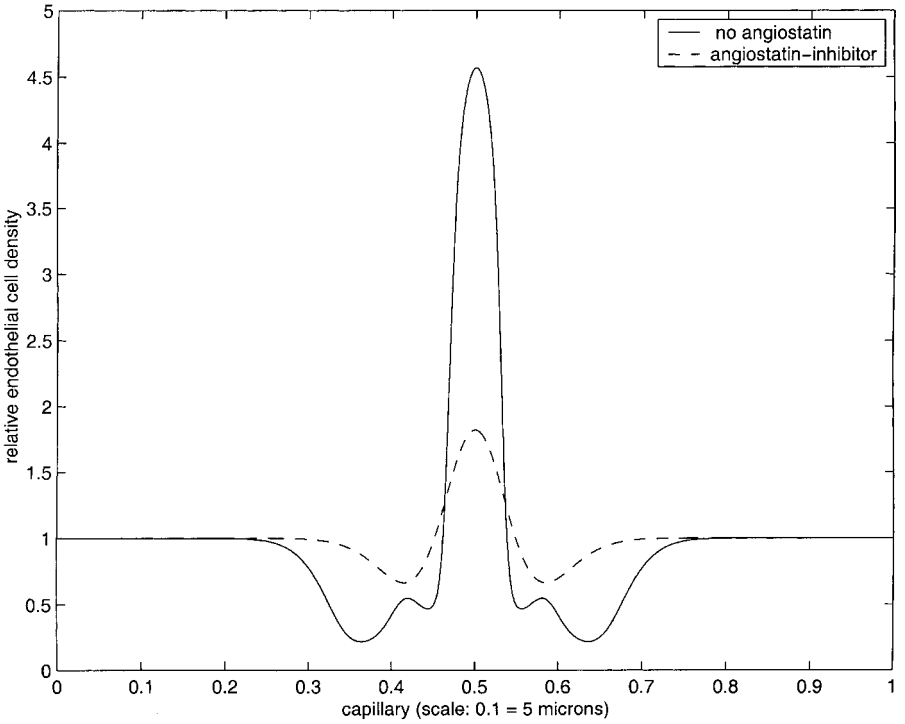

Fig. 11. Endothelial cell densities when $t = 0.10$ h.

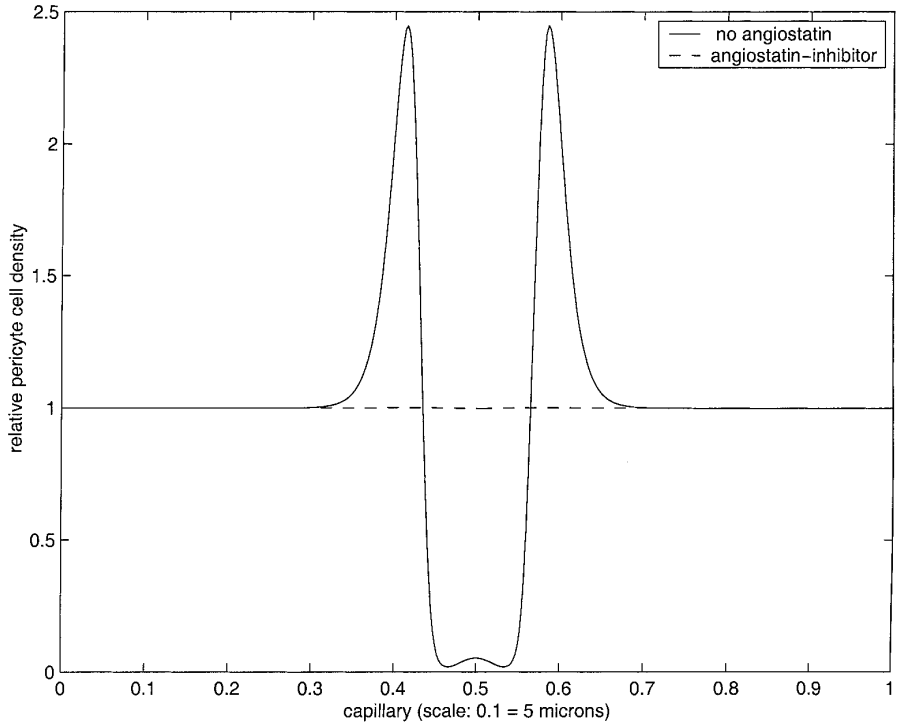

Fig. 12. PC densities when $t = 0.10$ h.

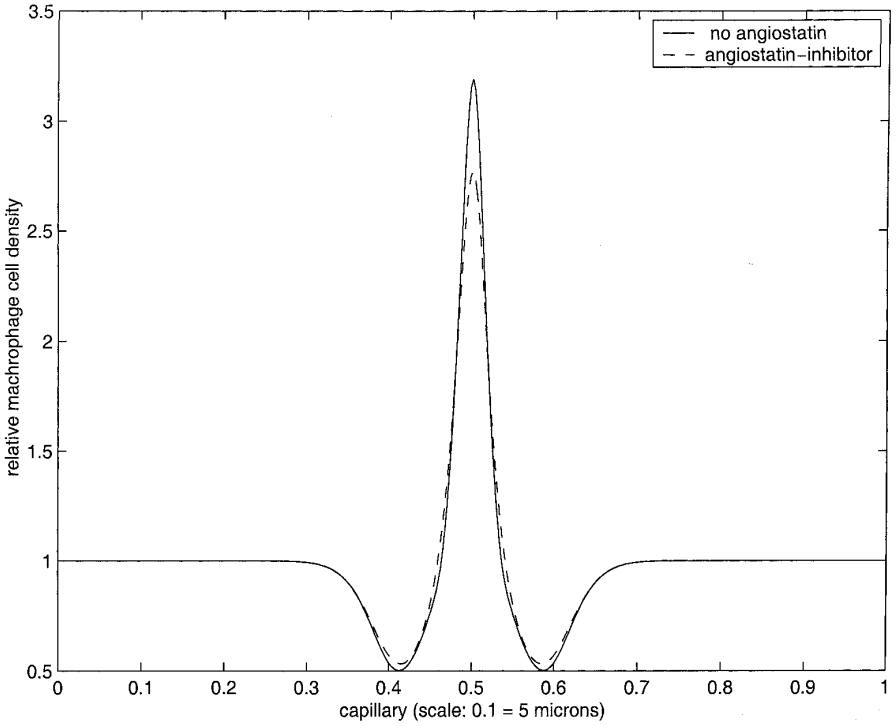

Fig. 13. Macrophage cell densities when $t = 0.10$ h.

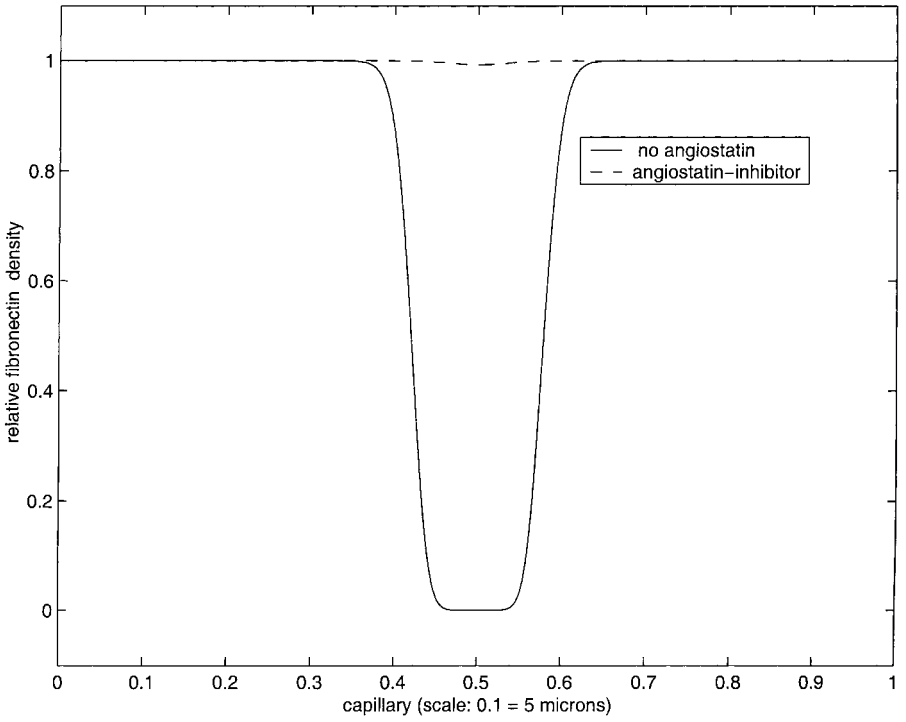

Fig. 14. Fibronectin densities when $t = 0.10$ h.

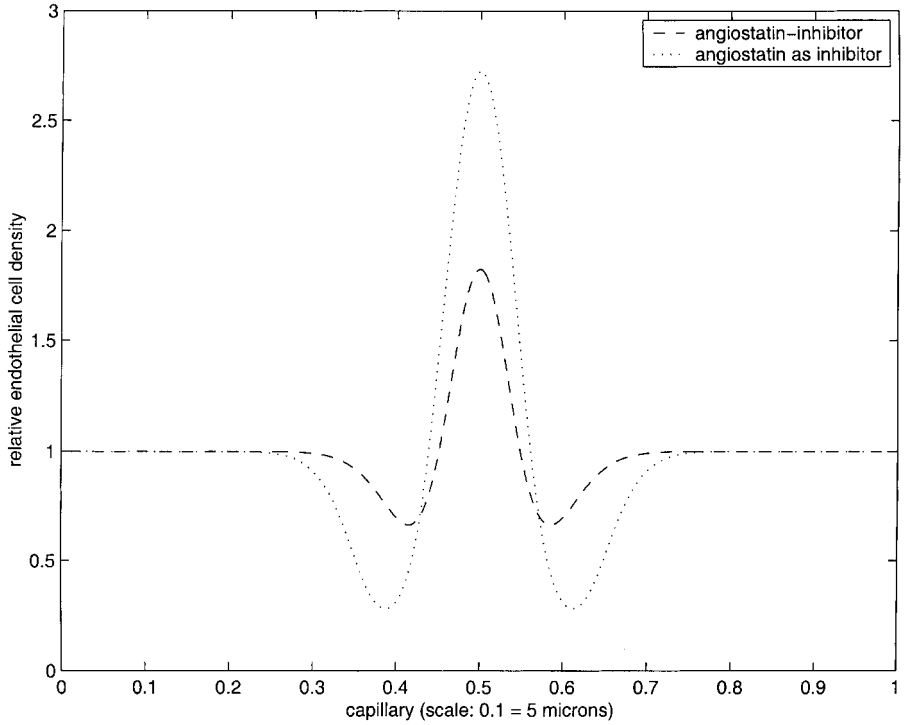

Fig. 15. Endothelial cell density for both the angiostatin mechanisms.

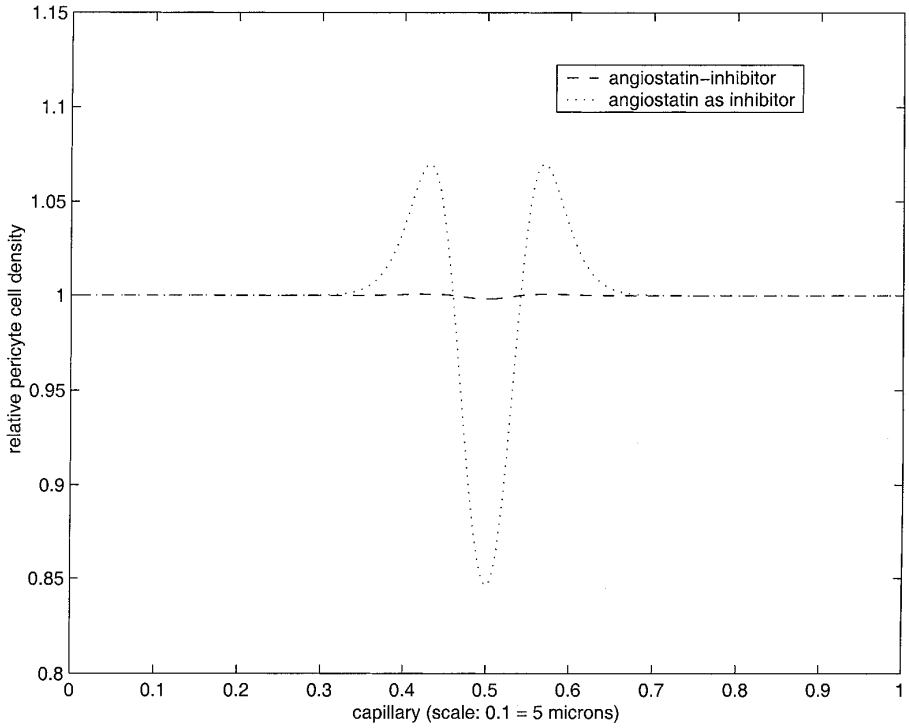

Fig. 16. PC density for both the angiostain mechanisms.

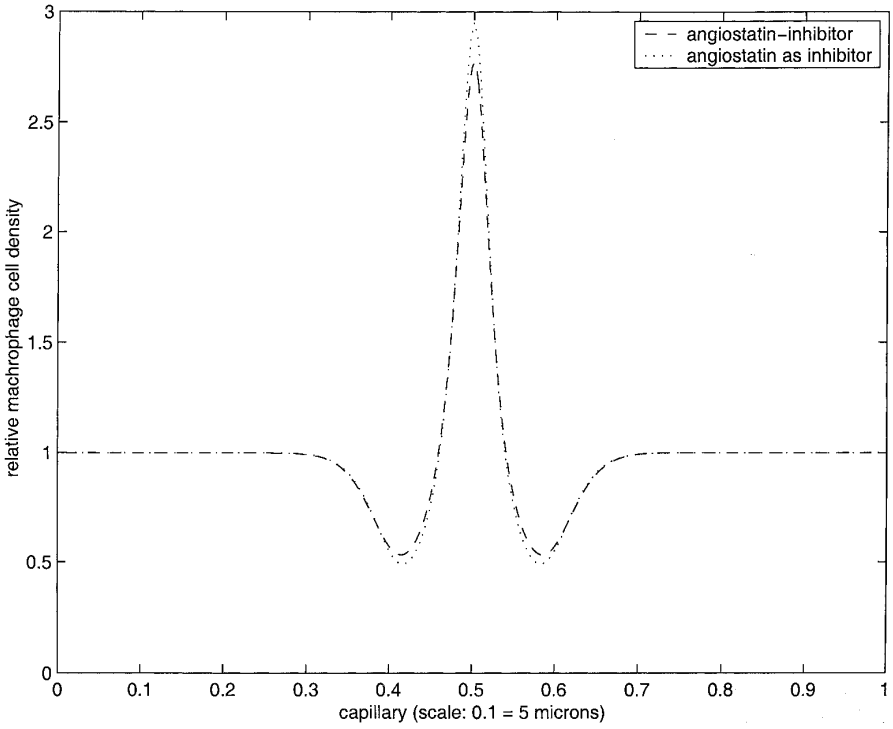

Fig. 17. Macrophage cell density for both the angiostatin mechanisms.

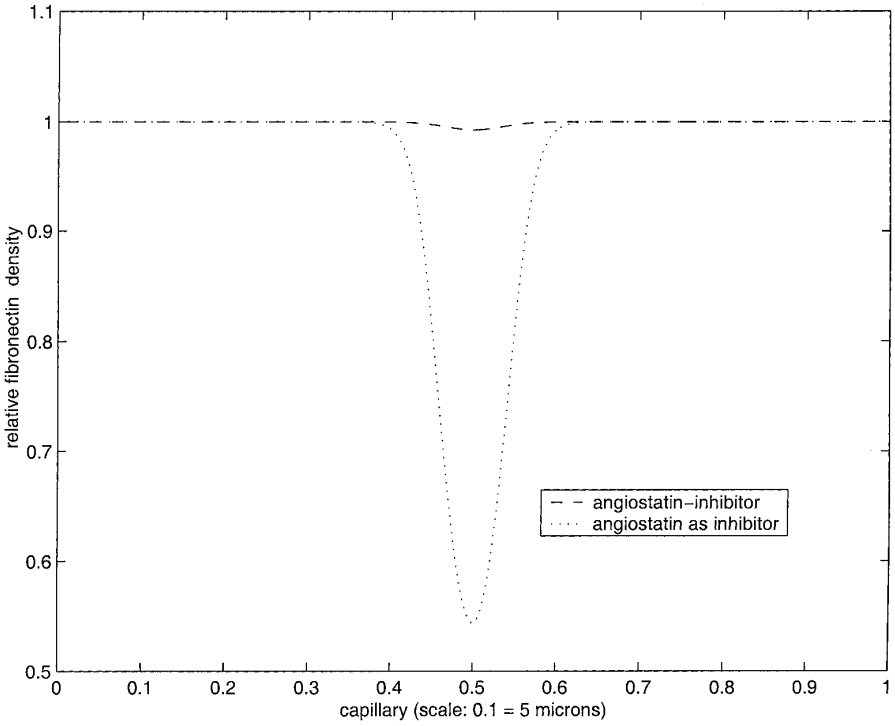

Fig. 18. Fibronectin density for both the angiostatin mechanisms.

(numerical) experiments (not shown) for large u_0, the former two cell types will exhibit bimodal distributions also.

In Fig. 9, we note the formation of an opening in the basement lamina as time evolves as measured by decreased fibronectin density near $x = 0.5$. Notice that the width of the opening near the minimum of the fibronectin is in the range 5–10 μm. (This can be made narrower by increasing the power m in the chemotactic source term. This narrows the support of $u_r(x,t)$ in x.)

In Fig. 10, we have plotted the fibronectin relative density profile along with the cell density profiles for EC, pericytes and MCs near the solution breakdown time. Notice that the pericyte aggregation in the opening in the capillary wall (the interval where $f < 1$) is low where the EC concentration is high and conversely. In particular, the maximum of PC density is higher closer to the wall of the forming capillary than is the maximum of the endothelial cell density. This is consistent with the observations of [30] that the PCs closely regulate the development of the forming channel.

In Figs. 11–14, we have plotted the final time profiles for the cell densities and fibronectin without and with angiostatin present in the case for which angiostatin produces an inhibitor. In Figs. 15–18, we compare the two mechanisms for the action of angiostatin.

In both sets of figures, we see that angiostatin inhibits endothelial and PC aggregation as well as fibronectin degradation. We understand this mathematically as follows.

From the differential equations (2.4.11) with (3.1)–(3.9), the angiostatin–inhibitor system, we see that if angiostatic agent is introduced into the system at a constant rate, then the inhibitor, ι_a, is increasing as a function of time. Since v_e is a large constant, very little active enzyme can be produced in the presence of angiostatic agent. When angiostatin acts as the inhibitor directly, its concentration increases linearly with time, if supplied at a constant rate A. On the other hand, the total number of macrophage and endothelial cells are fixed in this model, and therefore the total quantity of enzyme being produced by the endothelial cells is unchanged whether or not angiostatic agent is present.

Mathematically, what is occuring here is that in the fibronectin production equation, the dissipation term $-\lambda_4 c_a f/(1+v_4 f)$ will become small in comparison with the first, or fibronectin production rate, term. The effect of this is to prevent movement and aggregation of the endothelial cells so that the EC density, η, likewise returns to equilibrium (as does the PC density, ρ.) (Consider what happens in the extreme case when $v_e = +\infty$ so that the the equilibrium between C_A and C_I is completely to the C_I side. Then fibronectin cannot decay at all since there is no active enzyme to act as a catalyst of its decay.)

However, the presence of angiostatin has almost no effect on the distribution of macrophage cells since the inhibitor does not interfere with the chemotactic factor (see Figs. 13 and 17).

Moreover, when angiostatin produces inhibitor, it appears to be more effective in redistributing endothelial and pericyte cells and in returning the fibronectin to a uniform profile than when it acts as an inhibitor, even when the dosage rate is much larger in the latter case. The explanation for this lies in the observation that the equilibrium constant, v_3, is more than 1000 times larger in the former case than in the latter so that in the former case the efficiency with which c_a is inhibited is much greater.

As long as there is chemotactic factor being produced, one must continue to supply angiostatic agent 'therapy'. Thus, the treatment must be continued long enough for the tumor to effectively cease the production of chemotactic factor. Of course, if the half life of the chemotactic agent,

$\ln 2/\theta$, is small, then the effect of the angiostatic agent treatment will be much more pronounced. The inhibitor will convert all of the protease that can be generated by a finite quantity of chemotactic agent into the inactive state. We have shown this computationally but, for considerations of length, have not included the figures here.

In this paper, we have set out to develop as simple a model as possible to describe the initiation of capillary formation in tumor angiogenesis which includes the role of three of the important cellular players in these complex events. In particular we have extended our earlier model [18] to include the haptotactic saturation of fibronectin and the important roles played by PCs and MCs in regulating angiogenesis.

Computations based on this model are qualitatively consistent with experimental findings and clearly indicate one way in which the angiostatic agent can profoundly inhibit endothelial cell migration.

In summary, our modelling of the initiation of capillary sprout formation predicts that a unimodal stimulus of chemotactic factor (u_r) or angiogenic factor (v_r) induced directly by a tumor initiates a hole in the capillary wall (an opening for the nascent capillary) and a bi-modal distribution of endothelial cells in this nascent capillary sprout. This may be interpreted as a single opening leading to a sprout-like tube as shown in Fig. 1(c).

By attempting to model the presence of angiostatin, we have suggested two mechanisms by which the degradation of fibronectin is inhibited.

Finally, we highlight the fact that our modeling technique is quite general in that the dynamics of the chemical species (growth factor, protease, angiostatic agent, protease inhibitors, etc.) are firmly founded on the principles of chemical kinetics as they are expressed in Michaelis–Menten enzyme kinetics, while the cell movement equations are developed on the basis of the classical theory of reinforced random walks.

We are currently developing these ideas to model capillary formation and proliferation in the ECM. Preliminary computations with the extended model show that it can simulate anastamosis and vasculogenesis in addition to angiogenesis.

The whole process of angiogenesis is extremely complex. Nevertheless, we believe that our ideas represent a profound and fundamental step forward in the modeling of this process by providing a logical and biochemically based modeling procedure. We hope this model will improve the current state of understanding of this process, especially by giving some insight into how various growth inhibiting drugs (angiostatins) act to combat the progressively invasive disease of cancer. Likewise, by viewing the placenta as a 'tumor', we hope to obtain further insight into placental vascularization with this model.

Appendix A. The influence of VEGF diffusion

Another way to argue that we may neglect diffusion in growth factor transport in comparison to its conversion into protease is as follows: consider the case in which we have no chemotactic factor *or source term*. Including diffusion in the rate term for the v equation in (2.4.12), we write the rate equation for v in the form

$$v_t = D_v v_{xx} - \frac{\lambda_1 v \eta}{1 + \nu_1 v}.$$

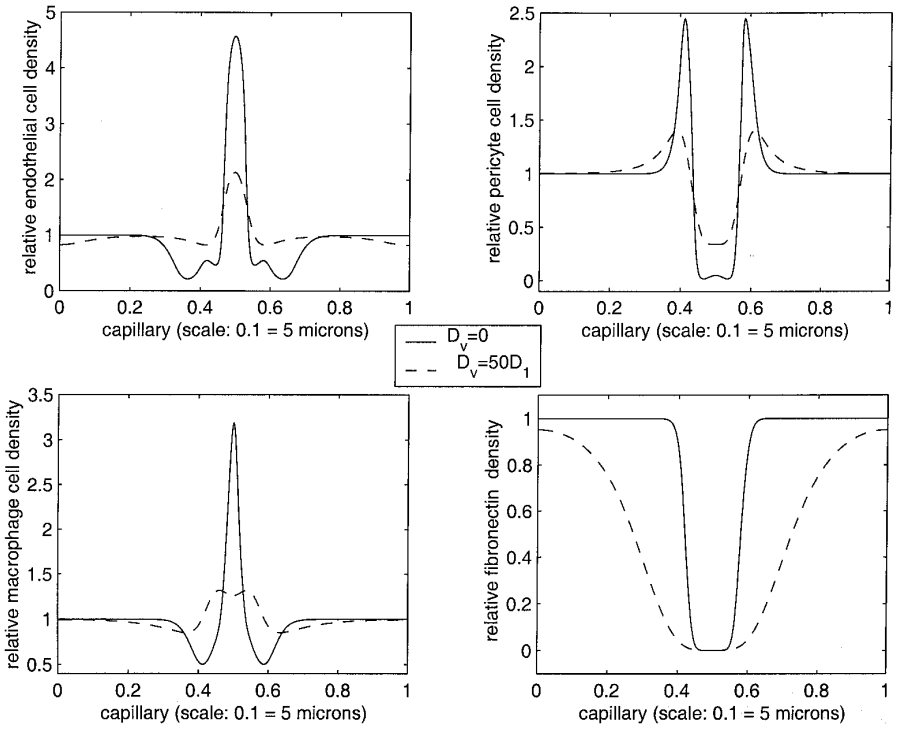

Fig. 19. No growth factor diffusion, growth factor diffusion at $t = 0.10$ h.

The time scale for the diffusion is L^2/D_v which is typically of order several hours [28]. Also, the decay of the fundamental solution of the diffusion equation is algebraic, like $(L^2t/D_v)^{-1/2}$. However the time scale for the second term is typically of order $1/(\lambda_1\eta_0) = K_m/(K_{\text{cat}}\delta\eta_0) \approx K_m/K_{\text{cat}}$, which is only of the order of seconds. [22] That is, if we write $v = we^{-\lambda_1\theta t}$, where $\theta < \eta_{\min}$ and $\eta_{\min} > 0$, then it is not too hard to see that $w_t \leqslant D_v w_{xx} + \lambda_1 w(\theta - \eta/(1 + vv_0))$, where $v(x,t) \leqslant v_0 \equiv \max v(x,0)$. (If $v_t(x,0) \leqslant 0$, and $v = 0$ at the ends of the interval, then v decreases, by the maximum principle.) If $\theta(1 + vv_0) < \eta_{\min}$, then w will likewise decay exponentially. Thus, the decay of v via chemistry is much faster than its decay via diffusion!

However, when we have a source term present, then one might argue that steep gradients induced by the source term, $u_r(x,t)$, might severely affect the capillary development. We show that this is only marginally true by considering the v equation in (2.4.12) to be of the form

$$v_t = D_v v_{xx} - \frac{\lambda_1 v\eta}{1 + v_1 v} + \frac{\lambda_2 u\eta}{1 + v_2 u}.$$

We have taken $D_v = 50D_1$, whereas in [28] an estimate is $D_v \approx 10^3 D_1$. We see from Fig. 19 that the diffusion term has the effect of broadening the capillary opening and producing

[22] For example, in [13], the vascular EC growth receptor KDR tyrosine kinase has a $K_m/K_{\text{cat}}\ \delta\eta_0$ value of about $130 \times 60/162 \approx 0.013$ h, whereas with $L = 2$ mm and $D_v = 10^{-7}$ cm^2/s [28], $L^2/D \approx 36$ h.

significantly more degradation in fibronectin due to the wider distribution of VEGF and hence of protease.

Notice that there is much less endothelial cell and PC aggregation and that the fibronectin channel is much less well defined. However, there is more chemotactic factor aggregation indicating a less efficient conversion of chemotactic factor into growth factor. The telling indicator that growth factor diffusion may be neglected is the size of the channel opening of the nascent capillary. Capillaries have diameters 7–8 μm with which our computations are consistent when growth factor diffusion is neglected. When it is included, even with D_v as small as $50D_1$, the predicted capillary opening is inconsistent with actual capillary diameters.

References

[1] R. Anderson, Mammary gland, in: B. Larson (Ed.), Lactation, Iowa State University, Ames, 1985, p. 1.
[2] A.R.A. Anderson, M.A.J. Chaplain, Modelling the growth and form of capillary networks, in: M.A.J. Chaplain, G.G. Singh, J.C. McLachlan (Eds.), On Growth and Form: Spatio-Temporal Pattern formation in Biology, Wiley, New York, 1999, p. 225.
[3] D.H. Ausprunk, J. Folkman, Migration and proliferation of endothelial cells in performed and newly formed blood vessels during tumor angiogenesis, Microvasc. Res. 14 (1977) 65.
[4] V. Ankoma-Sey, M. Matli, K.B. Chang, A. Lalazar, D.B. Donner, L. Wong, R.S. Warren, S.L. Friedman, Coordinated induction of VEGF receptors in mesenchymal cell types during rat hepatic wound healing, Oncogene 17 (1008) 115.
[5] J.C. Bowersox, N. Sorgente, Chemotaxis of aortic endothelial cells in response to fibronectin, Cancer Res. 4 (1982) 2547.
[6] D.J. Crocker, T.M. Murad, J.C. Geer, The role of the pericyte in wound healing: an ultra-structural study. Exp. Molec. Pathol. 13 (1970).
[7] B. Davis, Reinforced random walks, Prob. Theory Rel. Fields 84 (1990) 203.
[8] J. Folkman, Angiogenesis-retrospect and outlook, in: R. Steiner, P.B. Weisz, R. Langer (Eds.), Angiogenesis: Key Principles – Science – Technology – Medicine, Birkhäuser, Basel, 1992.
[9] G. Fields, S.J. Netzewl-Arnett, L.J. Windsor, J.A. Engler, H. Berkedal-Hansen, H.E. van Wart, Proteolytic activities of human fibroblast collagenaise, hydrolysis of a broad range of substrates at a single active site, Biochemistry 29 (1990) 6600.
[10] K.B. Glaser, L. Pease, J. Li, D.W. Morgan, Enhancement of the surface expression of tumor necrosis factor alpha (TNF-α) but not the p55TNF-α receptor in the THP-1 monocytic cell line by matrix metalloprotease inhibitors, Pharmacology 57 (1999) 291.
[11] D. Hanahan, J. Folkman, Patterns and emerging mechanisms of the angiogenic switch during tumorigenesis, Cell 86 (1996) 353.
[12] T. Kabelic, S. Ganbisa, B. Glaser, L.A. Liotta, Basement membrane collagen: degradation by migrating endothelial cells, Science 221 (1983) 281.
[13] R.L. Kendall, R.Z. Rutledge, X. Mao, A.J. Tebben, R.W. Hungate, K.A. Thomas, Vascular endothelial growth factor receptor KDR tyrosine kinase activity is increased by autophosporilation of two activation loop tyrosine residues, J. Biol. Chem. 274 (1999) 6453.
[14] A. Kuliopulos, L. Covic, S.K. Seeley, P.J. Sheridan, J. Helin, C.E. Costello, Plasmin desensitization of the PAR1 thrombin receptor: kinetics, sites of truncation, and implications for thrombolytic therapy, Biochemistry 38 (14) (1999) 4572.
[15] M. Kuwano, S. Ushiro, M. Ryuto, K. Samoto, H. Izumi, K. Ito, T. Abe, T. Nakamura, M. Ono, K. Kohno, Regulation of angiogenesis by growth factors, GANN Monograph Cancer Res. 42 (1994) 113.
[16] H.A. Levine, B.D. Sleeman, M. Nilsen-Hamilton, Mathematical modeling of capillary formation and development in tumor angiogenesis (manuscript).

[17] H.A. Levine, B.D. Sleeman, A system of reaction diffusion equations arising in the theory of reinforced random walks, SIAM J. Appl. Math. 57 (1997) 683.
[18] H.A. Levine, B.D. Sleeman, M. Nilsen-Hamilton, Mathematical modeling of the onset of capillary formation initiating angiogenesis, J. Math. Biol. (in press).
[19] J.D. Murray, Mathematical Biology, Biomathematics Texts, Springer, New York, 1989.
[20] N.J. Nelsen, Inhibitors of angiogenesis enter phase III testing, J. Nat. Cancer Inst. 90 (13) (1998) 960.
[21] R.M. Nerem, M.J. Levesque, J.F. Cornhill, Vasuclar endothelial cell morphology as an indicator of the pattern of blood flow, J. Biomech. Eng. 103 (3) (1981) 172.
[22] M.E. Orme, M.A.J. Chaplain, A mathematical model of the first steps of tumour related angiogenesis: capillary sprout formation and secondary branching, IMAJ Math. Appl. Med. Biol. 13 (1996) 73.
[23] H.G. Othmer, A., Stevens, Aggregation, blow up and collapse: the ABC's of taxis and reinforced random walks, SIAM J. Appl. Math. 57 (1997) 1044.
[24] N. Paweletz, M. Knierim, Tumor related angiogenesis, Crit. Rev. Oncol. Hematol 9 (1989) 197.
[25] K. Rakusan, Coronary angiogenesis. From morphology to molecular biology and back, Ann. NY Acad. Sci. 752 (1995) 257.
[26] B.D. Sleeman, Solid tumour growth: a case study in mathematical biology, in: P.J. Aston (Ed.), Nonlinear Mathematics and its Applications, Cambridge University, Cambridge, 1996, p. 237.
[27] M.S. Stack, S. Gately, L.M. Bafetti, J. Enghild, J. Spff, G.A. Soff, Angiostatin inhibits endothelial and melanoma cellular invasion by blocking matrix-enhanced plasminogen activation, Biochem. J. 340 (1999) 77.
[28] J.A. Sherrat, J.D. Murray, Models of epidermal wound healing, Proc. R. Soc. Lond. B 241 (1990) 19.
[29] J.A. Sherratt, A.J. Perunpanani, M.R. Owen, Pattern formation in cancer, in: M.A.J. Chaplain, G.G. Singh, J.C. McLachlon (Eds.), On Growth and Form: Spatio-Temporal Pattern formation in Biology, Wiley, New York, 1999, p. 747.
[30] A.M. Schor, A.E. Canfield, A.B. Sutton, T.D. Allen, P. Sloan, S.L. Schor, R. Steiner, P.B. Weisz, R. Langer, The behavior of pericytes in vitro: relevance to angiogenesis and differentiation, Angiogenesis: Key Principles – Science – Technology – Medicine, Birkhäuser, Basel, 1992.
[31] V.P. Terranova, R. DiFlorio, R.M. Lyall, S. Hic, R. Friesel, T. Maciag, Human endothelial cells are chemotactic to endothelial cell growth factor and heparin, J. Cell Biol. 101 (1985) 2330.
[32] K. Takahashi, H.C. Kwaan, E. Koh, M. Tanabe, Enzymatic properties of the phosphorylated urokinase-type plasminogen activator isolated from a human carcinomatous cell line, Biochem. Biophys. Res. Commun. 182 (1992) 1473.
[33] K.M. Yamada, K. Olden, Fibronectins-adhesive glycoproteins of cell surface and blood Nature 275 (1978) 179.
[34] J. Waltenberger, L. Claesson-Welsh, A. Siegbahn, M. Shibuya, C.-H. Heldin, Different signal transduction properties of KDR and Flt1, two receptors for vascular endothelial cell growth factor, J. Biol. Chem. 269 (1994) 26988.